

YITP-SB-99-15

INLO-PUB-12/99

Comparison between variable flavor number schemes for charm quark electroproduction

A. Chuvakin, J. Smith

C.N. Yang Institute for Theoretical Physics,

State University of New York at Stony Brook, New York 11794-3840, USA.

W. L. van Neerven

Instituut-Lorentz, University of Leiden, P.O. Box 9506, 2300 RA Leiden,
The Netherlands.

October 1999

Abstract

A comparison is made between two variable flavor number schemes which describe charm quark production in deep inelastic electron-proton scattering. In these schemes the coefficient functions are derived from mass factorization of the heavy quark coefficient functions presented in a fixed flavor number scheme. Since the coefficient functions in the variable flavor number schemes have to be finite in the limit $\mu \rightarrow 0$ we have defined a prescription for those processes where the virtual photon is attached to a light quark. Furthermore one has to construct a parton density set with four active flavors (u, d, s, c) out of a set which only contains three light flavors (u, d, s). In order to μ^2 the two sets are discontinuous at $\mu = m_c$ which follows from mass factorization of the heavy quark coefficient functions. The charm component of the structure function $F_{2,c}$ is insensitive to the different variable flavor number schemes. In particular in the threshold region they both agree with the description in fixed order perturbation theory presented in a three flavor scheme. However one version does not lead to a correct description of the threshold behavior of the longitudinal structure function $F_{L,c}$. This happens when one requires a non-vanishing zeroth order longitudinal coefficient function.

PACS numbers: 11.10Jj, 12.38Bx, 13.60Hb, 13.87Ce.

1 Introduction

Charm quark production is one of the important reactions used to extract the gluon density $f_g(x; Q^2)$ of the proton in deep inelastic lepton-hadron scattering, especially when the Bjorken scaling variable x is small. However this is only true when the deep inelastic process is of the neutral current type and the charm component of the proton wave function is negligible. In this case the charm quark is produced in the so-called extrinsic way. For neutral current processes with only light partons in the initial state this means that the Born approximation in perturbative QCD is given by the virtual vector-boson gluon-fusion process [1]. Notice that the light partons consist of the gluon and the three light flavors u, d, s together with their anti-particles. Furthermore if the virtuality of the exchanged vector boson in deep inelastic lepton-hadron scattering satisfies $Q^2 \gg M_Z^2$ then the vector boson is represented by the photon only and the contribution of the Z -boson is negligible. Extrinsic charm production also receives next-to-leading order (NLO) contributions from boson-quark subprocesses, which could hamper the extraction of the gluon density. Fortunately this is not the case at HERA, where the experiments [2], [3] are carried out at small x , because the gluon density overwhelms the light flavor densities completely. Moreover the NLO quark initiated processes are suppressed by at least one power of the strong coupling constant $\alpha_s(Q^2)$ with respect to the Born contribution to the boson-gluon fusion reaction. The quantity α_s in the running coupling constant and the parton densities represents both the renormalization and factorization scales respectively, because it is convenient to choose them to be equal.

In the literature one has adopted two different treatments of extrinsic charm production, which are known as the massive and massless charm descriptions. The former, advocated in [4], treats the charm quark as a heavy quark (with mass m_c) and the cross sections or coefficient functions have to be described by fixed order perturbation theory. Notice that due to the work in [5] the perturbation series is now known up to second order and the NLO massive charm approach agrees with the recent data in [2] and [3]. The latter treatment, which has been rather popular among groups which fitted parton densities to experimental data, treats the charm quark as a massless quark so that it can be represented by a parton density $f_c(x; Q^2)$, with the boundary condition $f_c(x; Q^2) = 0$ for $x \ll m_c$. Although at first sight these approaches are completely different they are actually intimately

related. It was shown in [6] that the large logarithms of the type $\ln(Q^2/m_c^2)$, which appear in the perturbation series when $Q^2 \ll m_c^2$, can be resummed in all orders. The upshot of this procedure is that the charm components of the deep inelastic structure functions $F_{i;c}(x;Q^2; m_c^2)$, where $i = 2; L$, which in the first approach are written as convolutions of heavy quark coherent functions with light parton densities, become, after resummation, convolutions of light parton coherent functions with light parton densities which also include a charm quark density. This procedure leads to the so-called zero mass variable flavor number scheme (ZM-VFNS) for $F_{i;c}(x;Q^2)$ where the mass of the charm quark is absorbed into the new four flavor densities. To implement this scheme one has to be careful to use quantities which are collinearly finite in the limit $m_c \rightarrow 0$. From the above considerations it is clear that the first approach is better when the charm quark pair is produced near threshold because the mass of the quark is important in this region and it cannot be neglected. On the other hand far away from threshold, where also $Q^2 \gg m_c^2$, the large logarithms above dominate the structure functions so that the second approach should be more appropriate. Both approaches are characterized by the number of active flavors involved in the description of the parton densities which are given by three and four respectively. Therefore one can also speak of three and four flavor number schemes (TFNS and FFNS respectively). Each scheme has a different gluon density so that the momentum sum rule is always satisfied.

As most of the experimental data occur in the kinematical regime which is between the threshold and the region of large Q^2 a third approach has been introduced to describe the charm components of the structure functions. This is called the variable flavor number scheme (VFNS). A first discussion was given in [7], where a VFNS prescription was given in lowest order only. A proof of factorization to all orders was recently given in [8], but the NLO expressions in this scheme were not provided. We will give them in this paper. A different approach, also generalized to all orders, was given in [6], [9]. Finally a third version of a VFNS was presented in [10]. The differences between the three versions can be attributed to two ingredients entering the construction of a VFNS. The first one is the mass factorization procedure carried out before the large logarithms can be resummed. The second one is the matching condition imposed on the charm quark density, which has to vanish in the threshold region of the production process. It will be one of our goals to elucidate these differences in the next Section. Another problem,

which was not clarified in the papers above is that the mass factorization cannot be carried out on the level of the charm components of the structure functions alone, because one also needs contributions coming from the light parton components of the structure functions. The latter can be attributed to all heavy charm quark loop contributions to gluon selfenergies, which appear in the virtual corrections to the light parton coefficient functions. These corrections have to be combined with contributions from gluon splitting into heavy charm anti-charm quark pairs, which belong to the charm components (not the light quark components) of the structure functions. In this paper we will give a much more careful analysis than has been done previously in the literature. Another aspect of any VFN S approach is that one needs two sets of parton densities. One set only contains densities in a three flavor number scheme whereas the second one, which also includes a charm quark density, is parameterized in a four flavor number scheme. Both parameterizations have to satisfy the relations quoted in [6]. At this moment the latter set is not available in the literature and we would like to fill in this gap. Starting from a three flavor number set of parton densities recently published in [11] we will construct a four flavor number set of densities satisfying the relations in [6].

In Sec. II we give a general discussion of the VFN S description for heavy quark electroproduction, and explain the problems with mass factorization, collinear singularities and threshold dependence in the heavy flavor component of the structure function. We then specialize to charm quark electroproduction in Sec. III, working to second order in the running coupling constant $\alpha_s(\mu^2)$. We first present details about the charm quark density. Next numerical results are shown for the structure functions in the various schemes. Analytic results for the contributions from the Compton scattering reaction with an invariant mass cut are relegated to an Appendix.

2 Discussion of variable flavor number schemes

In this section we discuss two different representations of the deep inelastic structure functions in variable flavor number schemes. One was proposed in [7], [8] and a version of it was used [10]. The other was proposed in [6] and [9]. The former starts from mass factorization of the exact heavy quark coefficient functions whereas the latter only applies this procedure to the asymptotic expressions for these functions. In both schemes the special role of the heavy quark loop contributions to the light quark coefficient functions in combination with heavy quark production via gluon splitting was overlooked. This will be repaired in this paper. Furthermore in both schemes there is a lot of freedom in the choice of matching conditions, which are needed to connect the structure functions presented for n_f and $n_f + 1$ light flavors. Different matching conditions lead to different threshold behaviors, which have consequences for the description of the structure functions at small Q^2 and large x .

Limiting ourselves to electroproduction, where deep inelastic lepton-hadron scattering is only mediated by a photon, the light parton components of the structure functions are defined by

$$\begin{aligned}
 F_i^{\text{LIGHT}}(n_f; Q^2; m^2) = & \\
 \sum_{k=1}^{n_f} e_k^2 f_q^S(n_f; Q^2) & C_{i;q}^{PS} n_f; \frac{Q^2}{2} + C_{i;q}^{V\text{IRT};PS} n_f; \frac{Q^2}{m^2}; \frac{Q^2}{2} \\
 + f_g^S(n_f; Q^2) & C_{i;g}^S n_f; \frac{Q^2}{2} + C_{i;g}^{V\text{IRT};S} n_f; \frac{Q^2}{m^2}; \frac{Q^2}{2} \\
 + f_{k+k}(n_f; Q^2) & C_{i;q}^{NS} n_f; \frac{Q^2}{2} + C_{i;q}^{V\text{IRT};NS} n_f; \frac{Q^2}{m^2}; \frac{Q^2}{2}; \quad (2.1)
 \end{aligned}$$

where \star denotes the convolution symbol in the parton Bjorken scaling variable z . In this expression the $C_{i;k}$ ($i = 2; L; k = q; g$) denote the light parton coefficient functions and the e_k represent the charges of the light flavor quarks. The quantities $C_{i;k}^{V\text{IRT}}$ only contain the heavy quark loop contributions to the light parton coefficient functions. Furthermore $f_g^S(n_f; Q^2)$ stands for the gluon density while the singlet (S) and non-singlet (NS) light quark

densities, with respect to the $SU(n_f)$ flavor group, are defined by

$$\begin{aligned}
 f_{k+k} (n_f; \frac{Q^2}{2}) &= \tilde{f} (n_f; \frac{Q^2}{2}) + f_k (n_f; \frac{Q^2}{2}) \\
 f_q^S (n_f; \frac{Q^2}{2}) &= \sum_{k=1}^{n_f} f_{k+k} (n_f; \frac{Q^2}{2}) \\
 f_q^{NS} (n_f; \frac{Q^2}{2}) &= f_{k+k} (n_f; \frac{Q^2}{2}) - \frac{1}{n_f} f_q^S (n_f; \frac{Q^2}{2}); \quad (2.2)
 \end{aligned}$$

Finally we have set the factorization scale equal to the renormalization scale. The light parton coefficient functions have been calculated up to order $\frac{Q^2}{s}$ in [12]. The contributions to $C_{i,k}^{VIRT}$ appear for the first time in second order perturbation theory and can be found in [13]. For our further discussion it will be convenient to distinguish between the numbers of external and internal avors. The former refers to the number of light avor densities whereas the latter denotes the number of light avors in the quark loop contributions to the virtual corrections. They are not necessarily equal. Some of the coefficient functions have the external avor number as an overall factor. To explicitly cancel this factor we have defined the quark and gluon coefficient functions in Eq. (2.1) as follows

$$\begin{aligned}
 C_{i,q}^S (n_f; \frac{Q^2}{2}) &= C_{i,q}^{NS} (n_f; \frac{Q^2}{2}) + C_{i,q}^{PS} (n_f; \frac{Q^2}{2}); \\
 C_{i,q}^{PS} (n_f; \frac{Q^2}{2}) &= n_f C_{i,q}^{PS} (n_f; \frac{Q^2}{2}); C_{i,g}^S (n_f; \frac{Q^2}{2}) = n_f C_{i,g}^S (n_f; \frac{Q^2}{2}); \quad (2.3)
 \end{aligned}$$

where PS represents the purely singlet component. Hence the remaining n_f in the argument of the coefficient functions marked with a tilde denotes the number of internal avors. The same holds for the n_f in the parton densities. However the argument n_f in the structure functions is external and it refers to the number of parton densities appearing in their expressions. The parton densities satisfy the renormalization group equations. If we define

$$D \frac{\partial}{\partial} + (n_f; g) \frac{\partial}{\partial g}; \quad g = g(n_f; \frac{Q^2}{2}) \quad (2.4)$$

then

$$D f_q^{NS} (n_f; \frac{Q^2}{2}) = \frac{NS}{qq} (n_f; g) f_q^{NS} (n_f; \frac{Q^2}{2})$$



Figure 1: Lowest-order photon-gluon fusion process $\gamma + g \rightarrow Q + \bar{Q}$ contributing to the coefficient functions $H_{i,g}^{S,(1)}$.

$$D f_k^S (n_f; Q^2) = \sum_{k=1}^S f_q^S (n_f; Q^2) f_l^S (n_f; Q^2) \quad k; l = q; g \quad (2.5)$$

where $f_{k,l}$ represent the anomalous dimensions of the operators in the operator product expansion (OPE).

The heavy flavor components ($Q = c; b; t$; $Q = c; b; t$) of the structure functions F_2 and F_L arise from Feynman graphs with heavy flavors (Q and Q with mass m) in the final state and are given by

$$\begin{aligned} F_{i,Q}^{\text{EXACT}} (n_f; Q^2; m^2) = & \sum_{k=1}^{\#} e_q^2 f_q^S (n_f; Q^2) L_{i,q}^{\text{PS}} n_f; \frac{Q^2}{m^2}; \frac{Q^2}{2} \\ & + f_g^S (n_f; Q^2) L_{i,g}^{\text{PS}} n_f; \frac{Q^2}{m^2}; \frac{Q^2}{2} + f_{k+k}^S (n_f; Q^2) L_{i,k}^{\text{NS}} n_f; \frac{Q^2}{m^2}; \frac{Q^2}{2} \\ & + e_Q^2 f_q^S (n_f; Q^2) H_{i,q}^{\text{PS}} n_f; \frac{Q^2}{m^2}; \frac{Q^2}{2} + f_g^S (n_f; Q^2) H_{i,g}^{\text{PS}} n_f; \frac{Q^2}{m^2}; \frac{Q^2}{2}; \end{aligned} \quad (2.6)$$

where e_Q represents the charge of the heavy quark. Further $L_{i,k}$ and $H_{i,k}$ ($i = 2; L; k = q; g$) represent the heavy-quark coefficient functions which are exactly calculated order by order in perturbation theory. In Figs. 1-5 we have shown some of the Feynman diagrams contributing to the coefficient functions up to order $\frac{2}{s}$. Like in the case of the light-parton coefficient functions $C_{i,k}$ they can be split into (purely)-singlet and non-singlet parts. The distinction between $L_{i,k}$ and $H_{i,k}$ can be traced back to the different (virtual)

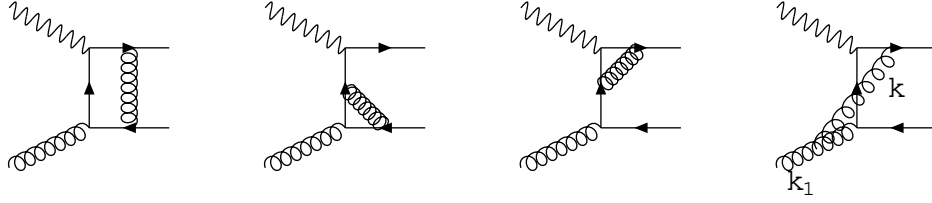


Figure 2: Virtual gluon corrections to the process $\gamma + g \rightarrow Q + \bar{Q}$ contributing to the coefficient functions $H_{i,g}^{S,(2)}$.

photon-parton heavy-quark production mechanisms from which they originate. The functions $L_{i,k}$, $H_{i,k}$ are attributed to the reactions where the virtual photon couples to the light quarks and the heavy quark respectively. Hence $L_{i,k}$ and $H_{i,k}$ in Eq. (2.6) are multiplied by e_k^2 and e_Q^2 respectively. As has been mentioned in the introduction the heavy quark coefficient functions contain large logarithms of the type $\ln^i(Q^2/m^2)$ when $Q^2 \ll m^2$ which can be removed from the former by using mass factorization. To do this we first have to split the heavy quark coefficient functions $L_{i,k}$ into soft and hard parts

$$L_{i,k}(n_f; \frac{Q^2}{m^2}; \frac{Q^2}{2}) = L_{i,k}^{\text{HARD}}(n_f; \frac{Q^2}{m^2}; \frac{Q^2}{2}) + L_{i,k}^{\text{SOFT}}(n_f; \frac{Q^2}{m^2}; \frac{Q^2}{2}); \quad (2.7)$$

where γ is a cut on the invariant mass s_{QQ} of the heavy quark pair. The cut is chosen in such a way that in the limit $m \rightarrow 0$ all mass singularities reside in the soft parts so that the hard parts are collinearly finite. Taking Fig. 5 as an example we mean by hard that one detects a $Q\bar{Q}$ -pair with a large invariant mass which is experimentally observable if $s_{QQ} > \gamma$. In the case $s_{QQ} < \gamma$ the $Q\bar{Q}$ -pair is soft and becomes indistinguishable from other light parton final states which contain contributions from virtual heavy quark loops. Next we add the soft parts to the other contributions to F_i^{LIGHT} in Eq. (2.1) and the mass factorization proceeds like

$$C_{i,k}(n_f; \frac{Q^2}{2}) + C_{i,k}^{\text{VIRT}}(n_f; \frac{Q^2}{m^2}; \frac{Q^2}{2}) + L_{i,k}^{\text{SOFT}}(n_f; \frac{Q^2}{m^2}; \frac{Q^2}{2}) =$$

$$\begin{aligned}
& A_{ik,Q} (n_f; \frac{Q^2}{m^2}) \quad C_{i,l} (n_f; \frac{Q^2}{2}) \\
& + A_{ik} (n_f; \frac{Q^2}{m^2}) \quad C_{i,l,Q}^{\text{V F N S; SOFT}} (n_f; ; \frac{Q^2}{m^2}; \frac{Q^2}{2}); \quad k;l = q;g; \quad (2.8)
\end{aligned}$$

Here $C_{i,l,Q}$ are those parts of the light parton coefficient functions $C_{i,l}$ which contain the heavy quark loops. The hard parts of $L_{i,k}$ are left in $F_{i,Q}^{\text{EXACT}}$ in Eq. (2.6) and do not need any mass factorization. Furthermore we have the condition that the dependence on the parameter μ cancels in the sums so

$$\begin{aligned}
C_{i,k,Q}^{\text{V F N S}} (n_f; \frac{Q^2}{m^2}; \frac{Q^2}{2}) &= C_{i,k,Q}^{\text{V F N S; SOFT}} (n_f; ; \frac{Q^2}{m^2}; \frac{Q^2}{2}) \\
&+ L_{i,k}^{\text{HARD}} (n_f; ; \frac{Q^2}{m^2}; \frac{Q^2}{2}); \quad (2.9)
\end{aligned}$$

where μ in the hard parts only represents the renormalization scale. The coefficient functions $H_{i,k}$ satisfy the relations

$$H_{i,k} (n_f; \frac{Q^2}{m^2}; \frac{Q^2}{2}) = A_{ik} (n_f; \frac{Q^2}{m^2}) \quad C_{i,l}^{\text{V F N S}} (n_f; \frac{Q^2}{m^2}; \frac{Q^2}{2}) \quad k;l = Q;g; \quad (2.10)$$

Notice that mass factorization applied to the functions $H_{i,Q}$ and $H_{i,g}$ occurring in $F_{i,Q}^{\text{EXACT}}$ (2.6) leads to the coefficient functions $C_{i,Q}^{\text{V F N S}}$. The latter also follow from mass factorization of the functions $H_{i,Q}$ which represent processes with a heavy quark in the initial state. The quantities $H_{i,Q}$, which do not appear in $F_{i,Q}^{\text{EXACT}}$, together with the corresponding operator matrix elements (OME's) $A_{Q,Q}$ are characteristic of variable flavor number schemes. The procedure above transfers the logarithms $\ln^i(\frac{Q^2}{m^2})$, appearing in $L_{i,k}^{\text{SOFT}}$ and $H_{i,k}$, to the heavy quark operator matrix elements $A_{ik,Q}$ and $A_{Q,k}$. The latter are defined by

$$\begin{aligned}
A_{ik,Q} &= h_k j O_1(0) j k i \quad k;l = q;g; \\
A_{Q,k} &= h_k j O_Q(0) j k i \quad k = Q;g; \quad (2.11)
\end{aligned}$$

Note that the O_1 are the light quark and gluon operators and in $A_{ik,Q}$ we only retain contributions from subgraphs which contain heavy quark (Q) loops. The quantity O_Q represents the heavy quark operator.

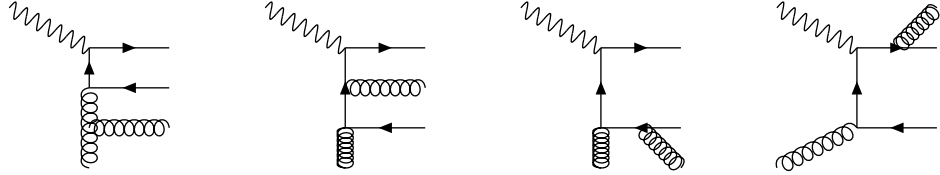


Figure 3: The bremsstrahlung process $\gamma + g \rightarrow Q + Q + g$ contributing to the coefficient functions $H_{i,g}^{S,(2)}$.

The heavy quark coefficient functions defined in the VFN S in Eqs. (2.8)–(2.10) are collinear finite and tend asymptotically to the massless parton coefficient functions presented in Eq. (2.1) i.e.

$$\lim_{Q^2 \rightarrow 1} C_{i,k}^{\text{VFN S}}(n_f; \frac{Q^2}{m^2}; \frac{Q^2}{2}) = C_{i,k}(n_f; \frac{Q^2}{2}); \quad k = Q; q; g; \quad (2.12)$$

In particular we have

$$C_{i,k}(n_f; \frac{Q^2}{2}) + \lim_{Q^2 \rightarrow m^2} C_{i,k,Q}^{\text{VFN S}}(n_f; \frac{Q^2}{m^2}; \frac{Q^2}{m^2}) = C_{i,k}(n_f + 1; \frac{Q^2}{2}); \quad (2.13)$$

so that the number of internal gluons is enhanced by one unit.

The VFN S above is similar to those proposed in [8], [10] except that the decomposition of the $L_{i,k}$ into soft and hard parts was ignored. However one cannot avoid this decomposition because the mass singularities in $L_{i,k}$ and $C_{i,k}^{\text{VIR}}$ separately have such high powers that they cannot be removed via mass factorization. Another feature is that in the limit $m \rightarrow 0$ the final state invariant energies in the reactions which contribute to these two types of coefficient functions become equal. Hence $L_{i,k}$ and $C_{i,k}^{\text{VIR}}$ have to be added so that the leading singularities cancel and the remaining ones are removed by mass factorization according to Eq. (2.8). On the other hand the total coefficient functions $L_{i,k}$ should not be moved to F_i^{LIGHT} . This would contradict the definitions of the latter structure functions where only light partons are observed in the final states. Therefore it is sufficient to transfer the $L_{i,k}^{\text{SOFT}}$ to the F_i^{LIGHT} since they contain the same mass singularities as the $L_{i,k}$. If m is chosen small enough, the heavy quarks are unobservable in a measurement of F_i^{LIGHT} .

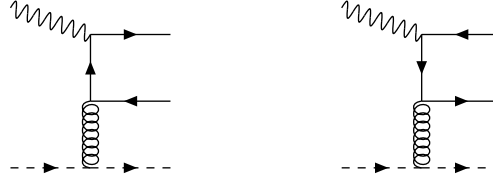


Figure 4: Bethe-Hetler process $+ q(\bar{q}) \rightarrow Q + \bar{Q} + q(\bar{q})$ contributing to the coefficient functions $H_{i;q}^{PS;(2)}$. The light quarks q and the heavy quarks Q are indicated by dashed and solid lines respectively.

To illustrate the procedure above we carry it out up to order $\frac{1}{s}$. The coefficients in the series expansion are defined as follows

$$C_{i;k} = \sum_{n=0}^{\frac{1}{s}} a_s^n C_{i;k}^{(n)} ; \quad H_{i;k} = \sum_{n=0}^{\frac{1}{s}} a_s^n H_{i;k}^{(n)} ; \quad L_{i;k} = \sum_{n=2}^{\frac{1}{s}} a_s^n L_{i;k}^{(n)} ;$$

$$A_{k;l} = \sum_{n=0}^{\frac{1}{s}} a_s^n A_{k;l}^{(n)} ; \quad \text{with} \quad a_s = \frac{s}{4} ; \quad (2.14)$$

Up to second order the mass factorization relations become

$$C_{i;q}^{VIRT\;NS;(2)} \left(\frac{Q^2}{m^2} \right) + L_{i;q}^{SOFT\;NS;(2)} ; \quad \frac{Q^2}{m^2} ; \frac{Q^2}{2} = A_{qqQ}^{NS;(2)} \frac{2}{m^2} C_{i;q}^{NS;(0)}$$

$$0 \not\propto \ln \frac{2}{m^2} C_{i;q}^{NS;(1)} \frac{Q^2}{2} + C_{i;qQ}^{VFN\;SOFT\;NS;(2)} ; \frac{Q^2}{m^2} ; \frac{Q^2}{2} ; \quad (2.15)$$

with

$$C_{i;q}^{VIRT\;NS;(2)} \left(\frac{Q^2}{m^2} \right) = F^{(2)} \left(\frac{Q^2}{m^2} \right) C_{i;q}^{(0)} ; \quad (2.16)$$

Here $F^{(2)}(Q^2 = m^2)$ denotes the two-loop vertex correction in Fig. 6. This function satisfies the decoupling theorem which implies that it vanishes in the limit $m \rightarrow 1$. The heavy quark coefficient functions $L_{i;k}^{NS;(2)}$ have been calculated in [14] and, after their convolution with the partonic densities,

yield contributions to the structure functions which behave asymptotically like $\ln^3(Q^2/m^2)$. These logarithms are canceled after adding $F^{(2)}(Q^2/m^2)$ in Ref. [13] to $L_{i,k}^{NS;SOFT;2}$ which contains the same mass singularities as $L_{i,k}^{NS;2}$ (see the remark below Eq. (2.7)). To obtain the hard and soft parts we divide the integral over $s_{Q\bar{Q}}$ in the graphs of Fig. 5 in two regions i.e. $s > s_{Q\bar{Q}} > \dots > s_{Q\bar{Q}} > 4m^2$ which we denote by HARD and SOFT respectively. Here $s_{Q\bar{Q}}$ and s denote the CM energies squared of the $Q\bar{Q}$ system and the incoming photon-parton state respectively. The hard and soft parts are presented in the Appendix. Finally $\alpha_Q = 2=3$ denotes the heavy quark contribution to the lowest order coefficient of the β -function in Eq. (2.4). We must change the running coupling constant when we change schemes.

The mass factorization of the heavy quark coefficient functions $H_{i,k}$ is simpler. Here we get

$$H_{i,q}^{PS;2} \frac{Q^2}{m^2}; \frac{Q^2}{2} = A_{Qq}^{PS;2} \frac{2}{m^2} C_{i,Q}^{VFNS;NS;0} \frac{Q^2}{m^2} + C_{i,q}^{VFNS;PS;2} \frac{Q^2}{m^2}; \frac{Q^2}{2}; \quad (2.17)$$

$$H_{i,Q}^{NS;1} \frac{Q^2}{m^2} = A_{Q\bar{Q}}^{NS;1} \frac{2}{m^2} C_{i,Q}^{VFNS;NS;0} \frac{Q^2}{m^2} + C_{i,Q}^{VFNS;NS;1} \frac{Q^2}{m^2}; \frac{Q^2}{2}; \quad (2.18)$$

$$H_{i,g}^{S;1} \frac{Q^2}{m^2} = A_{Qg}^{S;1} \frac{2}{m^2} C_{i,Q}^{VFNS;NS;0} \frac{Q^2}{m^2} + C_{i,g}^{VFNS;S;1} \frac{Q^2}{m^2}; \frac{Q^2}{2}; \quad (2.19)$$

$$H_{i,g}^{S;2} \frac{Q^2}{m^2}; \frac{Q^2}{2} = A_{Qg}^{S;2} \frac{2}{m^2} C_{i,Q}^{VFNS;NS;0} \frac{Q^2}{m^2} + C_{i,g}^{VFNS;S;2} \frac{Q^2}{m^2}; \frac{Q^2}{2} \\ + A_{Qg}^{S;1} \frac{2}{m^2} C_{i,Q}^{VFNS;NS;1} \frac{Q^2}{m^2}; \frac{Q^2}{2}; \quad (2.20)$$

In the expressions above we have only given the arguments on which the

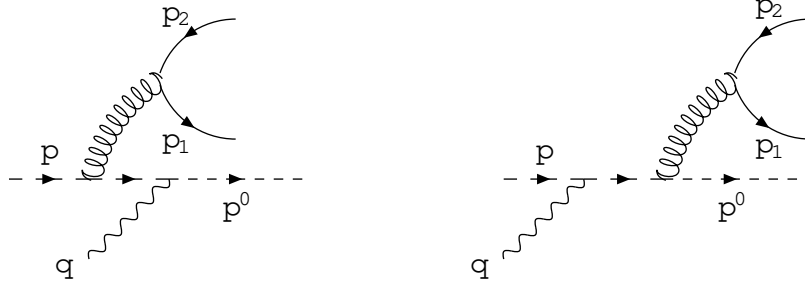


Figure 5: Compton process $(q) + q(p) \rightarrow Q(p_1) + Q(p_2) + q(p^0)$ contributing to the coefficient functions $L_{i,g}^{NS;(2)}$. The light quarks q and the heavy quarks Q are indicated by dashed and solid lines respectively ($s = (p+q)^2$, $s_{QQ} = (p_1+p_2)^2$ see text).

coefficient functions and operator matrix elements depend, like n_f , $Q^2 = m^2$, or $Q^2 = -2$ (at least up to that order in perturbation theory). Furthermore we have dropped the convolution symbol when the corresponding coefficient function behaves as a δ -function of the type $(1-z)$. The heavy quark coefficient functions correspond to the following processes

$$H_{i,g}^{S;(1)} : + g \rightarrow Q + Q \quad \text{Fig. 1}$$

$$H_{i,g}^{S;(2)} : + g \rightarrow Q + Q + g \quad \text{Figs. 2, 3}$$

$$H_{i,Q}^{PS;(2)} : + q(q) \rightarrow Q + Q + q(q) \quad \text{Fig. 4}$$

$$L_{i,q}^{NS;(2)} : + q(q) \rightarrow Q + Q + q(q) \quad \text{Fig. 5}$$

$$H_{i,Q}^{NS;(0)} : + Q \rightarrow Q$$

$$H_{i,Q}^{NS;(1)} : + Q \rightarrow Q + g \quad \text{Fig. 7:} \quad (2.21)$$

In the reactions above the virtual corrections to the lowest order processes are implicitly understood. The coefficient functions $L_{i,q}^{NS;(2)}$, $H_{i,Q}^{PS;(2)}$ and $H_{i,g}^{S;(2)}$ can be found in [5] whereas the $H_{i,Q}^{NS;(1)}$ are computed in the context of QED in [15]. A $A_{QQ}^{NS;(1)}$ in Eq. (2.18) is presented in the context of QED in [16] and

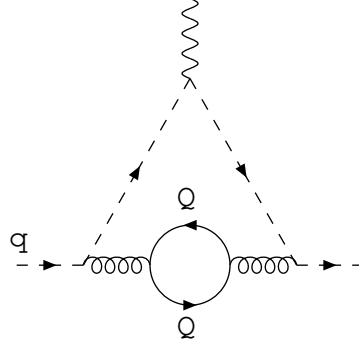


Figure 6: Two-loop vertex correction to the process $q + q \rightarrow q + q$ containing a heavy quark (Q) loop. It contributes to $C_{i,q}^{\text{VIRTA NS};(2)}(Q^2=m^2) = F^{(2)}(Q^2=m^2) C_{i,q}^{(0)}$.

the other OME's in Eqs. (2.15)–(2.20), which are also calculated up to second order, can be found in [6] and [14]. The mass singular logarithms of the type $\ln(Q^2/m^2)$, appearing in the OME's above, are absorbed by the light parton densities. This procedure leads to parton densities which are represented in the $n_f + 1$ flavor scheme. For the light parton densities one obtains

$$f_{k+k}(n_f + 1; Q^2) = A_{qgQ}^{\text{NS}} n_f; \frac{1}{m^2} \quad f_{k+k}(n_f; Q^2) + A_{qgQ}^{\text{PS}} n_f; \frac{1}{m^2} \\ f_q^S(n_f; Q^2) + A_{qgQ}^S n_f; \frac{1}{m^2} \quad f_g^S(n_f; Q^2); \quad k = 1 \quad f : n \quad (2.22)$$

The parton density representing the heavy quark in the $n_f + 1$ flavor scheme is

$$f_{Q+Q}(n_f + 1; Q^2) = A_{QgQ}^{\text{PS}} n_f; \frac{1}{m^2} \quad f_q^S(n_f; Q^2) \\ + A_{QgQ}^S n_f; \frac{1}{m^2} \quad f_g^S(n_f; Q^2); \quad (2.23)$$

Finally the gluon density in the $n_f + 1$ flavor scheme is

$$f_g^S(n_f + 1; Q^2) = A_{gqQ}^S(n_f; \frac{1}{m^2}) \quad f_q^S(n_f; Q^2)$$

$$+ A_{gg,Q}^S(n_f; \frac{2}{m^2}) \quad f_g^S(n_f; \frac{2}{m^2}); \quad (2.24)$$

One can check (see [6]) that the new parton densities satisfy the renormalization group equations in Eq. (2.5) wherein all quantities n_f are replaced by $n_f + 1$. Up to order a_s^2 the above relations become

$$f_{k+k}(n_f + 1; \frac{2}{m^2}) = f_{k+k}(n_f; \frac{2}{m^2}) + a_s^2(n_f; \frac{2}{m^2}) A_{qq,Q}^{NS;(2)} \frac{2}{m^2} f_{k+k}(n_f; \frac{2}{m^2}); \quad (2.25)$$

$$f_{Q+Q}(n_f + 1; \frac{2}{m^2}) = a_s(n_f; \frac{2}{m^2}) A_{Qg}^{S;(1)} \frac{2}{m^2} f_g^S(n_f; \frac{2}{m^2}) + a_s^2(n_f; \frac{2}{m^2}) A_{Qq}^{PS;(2)} \frac{2}{m^2} f_q^S(n_f; \frac{2}{m^2}) + A_{Qg}^{S;(2)} \frac{2}{m^2} f_g^S(n_f; \frac{2}{m^2}); \quad (2.26)$$

$$f_g^S(n_f + 1; \frac{2}{m^2}) = f_g^S(n_f; \frac{2}{m^2}) + a_s(n_f; \frac{2}{m^2}) A_{gg,Q}^{S;(1)} \frac{2}{m^2} f_g^S(n_f; \frac{2}{m^2}) + a_s^2(n_f; \frac{2}{m^2}) A_{gg,Q}^{S;(2)} \frac{2}{m^2} f_g^S(n_f; \frac{2}{m^2}) + A_{gg,Q}^{S;(2)} \frac{2}{m^2} f_g^S(n_f; \frac{2}{m^2}); \quad (2.27)$$

Notice that in passing from an n_f -avorto an $n_f + 1$ -avort scheme the running coupling constant becomes

$$a_s(n_f + 1; \frac{2}{m^2}) = a_s(n_f; \frac{2}{m^2}) \frac{h}{1 - a_s(n_f; \frac{2}{m^2}) \ln(\frac{2}{m^2})}; \quad (2.28)$$

which has to be used in all expressions for the structure functions in the VFNS. Using the mass factorization relations in Eqs. (2.8), (2.10) and the definitions of the parton densities in Eqs. (2.22)–(2.24) we obtain from Eq. (2.6) the heavy quark components of the structure functions in the VFNS

$$F_{iQ}^{\text{VFNS}}(n_f + 1; \frac{2}{m^2}) =$$

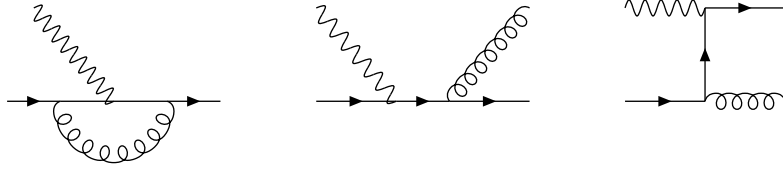


Figure 7: Order_s corrections to the process $+ Q \rightarrow Q$ and the reaction $+ Q \rightarrow Q + g$ contributing to the coefficient functions $H_{iQ}^{NS; (1)}$.

$$\begin{aligned}
 & \left. e_Q^2 f_{Q+Q} (n_f + 1; \frac{Q^2}{m^2}) \right. C_{iQ}^{VFNNS} (n_f + 1; \frac{Q^2}{m^2}; \frac{Q^2}{2}) \\
 & + C_{iQ}^{VFNPS} (n_f + 1; \frac{Q^2}{m^2}, \frac{Q^2}{2}) \\
 & + \sum_{l=1}^{X^f} f_{l+1} (n_f + 1; \frac{Q^2}{m^2}) C_{iQ}^{VFNPS} (n_f + 1; \frac{Q^2}{m^2}; \frac{Q^2}{2}) \\
 & + f_g^S (n_f + 1; \frac{Q^2}{m^2}) C_{iQ}^{VFNPS} (n_f + 1; \frac{Q^2}{m^2}; \frac{Q^2}{2}) \\
 & + \sum_{k=1}^{X^f} \sum_{l=1}^{X^f} e_k^2 f_{l+1} (n_f + 1; \frac{Q^2}{m^2}) L_{iQ}^{HARDPS} (n_f; \frac{Q^2}{m^2}; \frac{Q^2}{2}) \\
 & + f_g^S (n_f + 1; \frac{Q^2}{m^2}) L_{iQ}^{HARDPS} (n_f; \frac{Q^2}{m^2}; \frac{Q^2}{2}) \\
 & + f_{k+k} (n_f + 1; \frac{Q^2}{m^2}) L_{iQ}^{HARDPS} (n_f; \frac{Q^2}{m^2}; \frac{Q^2}{2}) \quad : \quad (2.29)
 \end{aligned}$$

In a similar way one obtains from Eq. (2.1) the light parton components of the structure functions in the VFN S

$$F_i^{VFNSLIGHT} (n_f; \frac{Q^2}{m^2}) = \sum_{k=1}^{X^f} e_k^2$$

$$\begin{aligned}
 & \sum_{l=1}^{N_f} f_{l+1}(n_f + 1; \frac{Q^2}{m^2}) \quad C_{iq}^{PS} n_f; \frac{Q^2}{m^2} + C_{iq;Q}^{VFNS;SOFT;PS} n_f; \frac{Q^2}{m^2}; \frac{Q^2}{m^2} \\
 & + f_g^S(n_f + 1; \frac{Q^2}{m^2}) \quad C_{iq}^S n_f; \frac{Q^2}{m^2} + C_{iq;Q}^{VFNS;SOFT;S} n_f; \frac{Q^2}{m^2}; \frac{Q^2}{m^2} \\
 & + f_{k+k}(n_f + 1; \frac{Q^2}{m^2}) \quad C_{iq}^{NS} n_f; \frac{Q^2}{m^2} + C_{iq;Q}^{VFNS;SOFT;NS} n_f; \frac{Q^2}{m^2}; \frac{Q^2}{m^2} \quad (2.30)
 \end{aligned}$$

Up to a given order Eqs. (2.29) and (2.30) do not differ from the structure functions presented in Eqs. (2.6) and (2.1) respectively as long as one uses fixed order perturbation theory. This can be checked up to second order when the coefficient functions in Eqs. (2.29) and (2.30) are substituted using the mass factorization relations in (2.15)–(2.20). The difference arises if the logarithms of the type $\ln^i(\lambda^2/m^2)$, which show up in the parton densities, are resummed using the renormalization group equations in Eq. (2.5). This resummation induces corrections beyond fixed order perturbation theory which become noticeable for $\lambda^2 \gg m^2$. On the other hand we do not want that the resummation bedevils the threshold behavior of the structure functions. In this region the best representation is still given by Eqs. (2.1) and (2.6). Therefore one has to look for a scale at which expressions (2.29) and (2.30) coincide with those given by fixed order perturbation theory in (2.6) and (2.1) respectively. Finding this scale is the most important issue in VFNS as we will show below. Both expressions F_{iQ}^{VFNS} and $F_i^{\text{VFNS, LIGHT}}$ are renormalization group invariants. Hence they satisfy the renormalization group equations (see Eq. (2.4))

$$D F_{iQ}^{VFNS} = 0; \quad D F_i^{VFNS, LIGHT} = 0; \quad (2.31)$$

The same holds for the total structure function in the variable flavor number scheme which is defined as

$$F_i^{VFNS}(n_f + 1; Q^2; m^2) = F_i^{VFNS, LIGHT}(n_f; ; Q^2; m^2) + F_{iQ}^{VFNS}(n_f + 1; ; Q^2; m^2); \quad (2.32)$$

One can now show that for large Q^2 , $F_i^{\text{VFNS}}(n_f + 1; Q^2; m^2)$ turns into the

same expression as Eq. (2.1) where n_f in the light parton coefficient functions $C_{i;k}^{\text{VFR}}$ is replaced by $n_f + 1$ and $C_{i;k}^{\text{VFR}} = 0$ for the $n_f + 1$ heavy flavor piece.

After having discussed the general procedure to construct VFNS structure functions we now turn to the practical issues. For asymptotic values of Q^2 , far above the heavy $Q\bar{Q}$ threshold at $(1-x)Q^2=x=4m^2$, all coefficient functions $C_{i;k}^{\text{VFNS}}$ in Eq. (2.29) can be replaced by the light parton coefficient functions so that, after having removed $L_{i;k}^{\text{HARD}}$, one gets the heavy quark components of the structure functions in the so-called zero mass variable flavor number scheme (ZM-VFNS). However near threshold at low Q^2 and large x there is a problem, which has not been solved satisfactorily in the literature. In this region one would like the $F_{i,Q}^{\text{VFNS}}$ to vanish in the same way that the $F_{i,Q}^{\text{EXACT}}$ vanish. Unfortunately the coefficient functions $C_{i,Q}^{\text{VFNS}}$ do not vanish in the threshold region due to the presence of the OEM's $A_{Q,k}^S$ and the functions $H_{i,Q}^N$ which describe processes with ONE heavy quark in the final state (see Eq. (2.21)) contrary to $H_{i,g}$ and $H_{i,q}$ which originate from reactions with at least TWO heavy quarks (Q and \bar{Q}) in the final state. Only the latter functions have the correct threshold behavior. In the literature two ways have been proposed to obtain reasonable threshold behaviors. The first one was given in a paper by Avanessian, Collins, Gross and Tung [7], which will be denoted as the ACOT boundary conditions. The second one was proposed in a paper by Thorne and Roberts [10], which we shall call the TR boundary conditions. In both approaches one requires the conditions

$$F_{i,Q}(Q^2; m^2) = F_{i,Q}^{\text{EXACT}}(n_f; Q^2; m^2) \quad \text{for } Q^2 < m^2;$$

$$F_{i,Q}(Q^2; m^2) = F_{i,Q}^{\text{VFNS}}(n_f + 1; Q^2; m^2) \quad \text{for } Q^2 > m^2; \quad (2.33)$$

where the parton densities satisfy the properties for $Q^2 > m^2$

$$f_{k+k}(n_f + 1; x; Q^2) = f_{k+k}(n_f; x; Q^2);$$

$$f_{Q+Q}(n_f + 1; x; Q^2) = 0;$$

$$f_g(n_f + 1; x; Q^2) = f_g(n_f; x; Q^2); \quad (2.34)$$

Notice that there is no relation between the scale μ chosen in these boundary conditions, and the production threshold of heavy quarks $(1-x)Q^2=x=4m^2$. If one e.g. takes $\mu^2 = Q^2$ and $Q^2 > m^2$ all terms in Eq. (2.29), where

the heavy quark density is multiplied with C_{iQ}^{VFNS} , vanish in spite of the fact that heavy avors are still produced as long as $x < Q^2 = (Q^2 + 4m^2)$. On the other hand it is possible that $Q^2 > m^2$ and $x = Q^2 = (Q^2 + 4m^2)$ which implies a non-vanishing heavy quark density with no heavy quark pair production. Another feature is that the boundary conditions above are at variance with the relations in Eqs. (2.22)–(2.24). Although up to order a_s all OME's in the $\overline{\text{MS}}$ -scheme vanish at $Q^2 = m^2$ this no longer holds when $Q^2 < m^2$. Furthermore (see [6]) the OME's do not vanish anymore at $Q^2 = m^2$ when they are calculated beyond one-loop order in the $\overline{\text{MS}}$ -scheme. Hence the threshold behavior of F_{iQ}^{VFNS} will be spoiled since $C_{i,k}^{\text{VFNS}} \notin H_{i,k}$ for $Q^2 < m^2$. In order to repair this ACO T proposed the prescription

$$Q^2 = m^2 + kQ^2 \quad 1 - \frac{m^2}{Q^2}^{!n} \quad \text{for } Q^2 > m^2;$$

$$Q^2 = m^2 \quad \text{for } Q^2 < m^2; \quad (2.35)$$

with $k = 1=2$ and $n = 2$. In this way one gets $C_{i,k}^{\text{VFNS}} = H_{i,k}$ for $Q^2 < m^2$ at least up to order a_s . For higher orders one has to use the relations in Eqs. (2.22)–(2.24) instead of those given in Eq. (2.34) as the latter only hold up to order a_s^2 . The new conditions are presented up to order a_s^2 in Eqs. (2.25)–(2.27).

In the TR prescription one chooses $Q^2 = Q^2$ and requires

$$F_i^{\text{VFNS}}(n_f + 1; Q^2; m^2) \Big|_{Q^2=m^2} = F_i^{\text{EXACT}}(n_f; Q^2; m^2) \Big|_{Q^2=m^2};$$

$$\frac{dF_i^{\text{VFNS}}(n_f + 1; Q^2; m^2)}{d \ln(Q^2=m^2)} \Big|_{Q^2=m^2} = \frac{dF_i^{\text{EXACT}}(n_f; Q^2; m^2)}{d \ln(Q^2=m^2)} \Big|_{Q^2=m^2}; \quad (2.36)$$

Using them ass factorization relations in Eqs. (2.17)–(2.20) the TR boundary conditions lead to new heavy quark coe cient functions C_{iQ}^{VFNS} which have nothing to do with the reactions in Eq. (2.21). For instance the lowest order coe cient functions in the TR prescription corresponding to the reaction $Q + Q \rightarrow Q + Q$ in Eq. (2.21) vanish at the QQ threshold although this process only contains one heavy quark in the nal state. Moreover, as already adm itted by the authors in [10], this procedure breaks down beyond order a_s because there are more coe cient functions than relations between them. Another

problem is that it is unclear in which subtraction scheme one is working since the subtraction terms in [10] have nothing to do with the usual OME's except in the limit $Q^2 \gg m^2$. For example in order a_s the subtraction term needed for $H_{iQ}^{NS;1}$ in Eq. (2.18) is not given by $A_{Qg}^{NS;1}$. The same holds for $H_{iQ}^{S;1}$ in Eq. (2.19), which gets another subtraction than given by $A_{Qg}^{S;1}$. From the theoretical viewpoint the boundary conditions in Eq. (2.36) seem very unattractive to us because the relations between the coefficient functions C_{ik}^{VFN} ($k = Q; q; g$) and the actual parton reactions are broken and the scheme is unknown. Notice that the parton densities in [10] are still presented in the \overline{MS} -scheme.

A different VFN S from those discussed above has been proposed by Buza, Matiounine, Smirnov and van Neerven in [6], [9], which we call the BM SN scheme. In the latter it was advocated that only when the large logarithms dominate the heavy quark coefficient functions do they have to be removed via mass factorization so that they can be resummed via the renormalization group equations. In the BM SN scheme we need the asymptotic heavy quark coefficient functions defined by

$$\lim_{Q^2 \gg m^2} H_{ik}(n_f; \frac{Q^2}{m^2}; \frac{Q^2}{2}) = H_{ik}^{\text{ASYM P}}(n_f; \frac{Q^2}{m^2}; \frac{Q^2}{2}); \quad (2.37)$$

which behave like

$$H_{ik}^{\text{ASYM P};1}(n_f; \frac{Q^2}{m^2}; \frac{Q^2}{2}) \underset{n+j=1}{\overset{1}{\sum}} a_{nj} \ln^n \frac{Q^2}{m^2} \ln^j \frac{Q^2}{2}; \quad (2.38)$$

with a similar behavior for $L_{ik}^{\text{ASYM P}}$. In the BM SN scheme F_{iQ}^{EXACT} is given by Eq. (2.6) except that $L_{ik} \neq L_{ik}^{\text{HARD}}$ analogous to the VFN S. The asymptotic heavy quark structure functions, denoted by $F_{iQ}^{\text{ASYM P}}$, are given by the same expressions as presented for F_{iQ}^{EXACT} where now all exact heavy quark functions are replaced by their asymptotic ones. Up to second order the latter can be found in [14]. The functions $L_{iQ}^{\text{SOFT ASYM PNS};2}$ and $L_{iQ}^{\text{HARD ASYM PNS};2}$ are given in Appendix A. In the BM SN scheme the charm components of the structure functions are defined as

$$\begin{aligned} F_{iQ}^{\text{BM SN}}(n_f + 1; \frac{Q^2}{m^2}) &= F_{iQ}^{\text{EXACT}}(n_f; \frac{Q^2}{m^2}) \\ F_{iQ}^{\text{ASYM P}}(n_f; \frac{Q^2}{m^2}) &+ F_{iQ}^{\text{PDF}}(n_f + 1; \frac{Q^2}{m^2}); \end{aligned} \quad (2.39)$$

with

$$\begin{aligned}
F_{iQ}^{PDF}(n_f + 1; Q^2; m^2) = & \\
& e_Q^2 f_q^S(n_f + 1; Q^2) C_{iq}^{PS} n_f + 1; \frac{Q^2}{2} + f_g^S(n_f + 1; Q^2) \\
& C_{iqg}^S n_f + 1; \frac{Q^2}{2} + f_{Q+Q}(n_f + 1; Q^2) C_{iq}^{NS} n_f + 1; \frac{Q^2}{2} \\
& + \sum_{k=1}^{n_f} \sum_{l=1}^{n_f} e_k^2 f_{l+1}(n_f + 1; Q^2) L_{iq}^{HARD ASYMP; S} n_f; \frac{Q^2}{m^2}; \frac{Q^2}{2} \\
& + f_g^S(n_f + 1; Q^2) L_{iqg}^{HARD ASYMP; S} n_f; \frac{Q^2}{m^2}; \frac{Q^2}{2} \\
& + f_{k+k}(n_f + 1; Q^2) L_{iq}^{HARD ASYMP; NS} n_f; \frac{Q^2}{m^2}; \frac{Q^2}{2} \quad ; \quad (2.40)
\end{aligned}$$

The structure functions F_{iQ}^{PDF} are obtained from the F_{iQ}^{ASYMP} via the mass factorization relations in Eqs. (2.7), (2.10) by making the replacements $H_{ik} \rightarrow H_{ik}^{ASYMP}$, $L_{ik} \rightarrow L_{ik}^{ASYMP}$ and $C_{ik}^{VFNS} \rightarrow C_{ik}^{ASYMP}$ on the left and right-hand sides respectively. Furthermore we have used the definitions for the parton densities in Eqs. (2.22)–(2.24). Notice that if the coefficient functions, indicated by $L_{ik}^{HARD ASYMP}$, are removed from F_{iQ}^{PDF} one obtains the structure functions in the ZM-VFNS. The light parton components of the structure functions become

$$\begin{aligned}
F_i^{BMSN; LIGHT}(n_f; Q^2; m^2) = & \\
& e_k^2 f_{l+1}(n_f + 1; Q^2) C_{iq}^{PS} n_f; \frac{Q^2}{m^2}; \frac{Q^2}{2} \\
& + f_g^S(n_f + 1; Q^2) C_{iqg}^S n_f; \frac{Q^2}{m^2}; \frac{Q^2}{2} \\
& + f_{k+k}(n_f + 1; Q^2) C_{iq}^{NS} n_f; \frac{Q^2}{m^2}; \frac{Q^2}{2} \quad ; \quad (2.41)
\end{aligned}$$

with

$$\begin{aligned}
 C_{i;k} \ n_f; ; \frac{Q^2}{m^2}; \frac{Q^2}{2} &= C_{i;k} \ n_f + 1; \frac{Q^2}{2} + C_{i;k}^{V\text{FT}} \ n_f; \frac{Q^2}{m^2}; \frac{Q^2}{2} \\
 &+ L_{i;k}^{\text{SOFT}} \ n_f; ; \frac{Q^2}{m^2}; \frac{Q^2}{2} - C_{i;k}^{V\text{FT ASYM}} \ n_f; \frac{Q^2}{m^2}; \frac{Q^2}{2} \\
 L_{i;k}^{\text{ASYM}} \ n_f; \frac{Q^2}{m^2}; \frac{Q^2}{2} &:
 \end{aligned} \tag{2.42}$$

The coefficient functions above satisfy the property that

$$\begin{aligned}
 \lim_{Q^2 \rightarrow m^2} C_{i;k} \ n_f; ; \frac{Q^2}{m^2}; \frac{Q^2}{2} &= \\
 C_{i;k} \ n_f + 1; \frac{Q^2}{2} - L_{i;k}^{\text{HARD ASYM}} \ n_f; ; \frac{Q^2}{m^2}; \frac{Q^2}{2} &:
 \end{aligned} \tag{2.43}$$

Using the relations in Eqs. (2.9), (2.12) one can make a comparison between the VFN S and the BM SN scheme. In the asymptotic limit the heavy quark components satisfy (see Eqs. (2.29), (2.39), (2.40))

$$\begin{aligned}
 \lim_{Q^2 \rightarrow m^2} F_{i;Q}^{\text{BM SN}} (n_f + 1; ; Q^2; m^2) &= \lim_{Q^2 \rightarrow m^2} F_{i;Q}^{\text{VFN S}} (n_f + 1; ; Q^2; m^2) \\
 &= \lim_{Q^2 \rightarrow m^2} F_{i;Q}^{\text{PDF}} (n_f + 1; ; Q^2; m^2);
 \end{aligned} \tag{2.44}$$

and the light parton components satisfy (see Eqs. (2.30), (2.41))

$$\lim_{Q^2 \rightarrow m^2} F_i^{\text{BM SN; LIG HT}} (n_f; ; Q^2; m^2) = \lim_{Q^2 \rightarrow m^2} F_i^{\text{VFN S; LIG HT}} (n_f; ; Q^2; m^2); \tag{2.45}$$

provided we impose the same boundary conditions on both schemes. From the discussion above we infer that the only difference between the VFN S and the BM SN scheme can be attributed to the $m^2 = Q^2$ -terms which are present in $C_{i;k}^{\text{VFN S}}$ but absent in $C_{i;k}$. In the next Section we will make a study where in Q^2 these differences are noticeable.

3 Comparison between the VFNS and the BM SN scheme

In this Section we will make a comparison in the case of charm production between the VFNS as proposed in [7], [8] and the BM SN scheme in [6], [9]. For that purpose we construct a parton density set with four active avors from an existing three avor set in the literature following Eqs. (2.22)–(2.24). The charm quark density of our set will be compared with those in other sets with four active avors presented in [17] (MRST 98, central gluon) and [18] (CTEQ 5HQ). Using our set we will study the differences between the charm components of the structure functions $F_{i;c}^{\text{VFNS}}(n_f + 1)$ in Eq. (2.29) and $F_{i;c}^{\text{BM SN}}(n_f + 1)$ in Eq. (2.39) in particular in the threshold region.

Since all coefficient functions are computed in the $\overline{\text{MS}}\text{-scheme}$ we choose the leading order (LO) and next-to-leading order (NLO) parton density sets presented in [11] which contain three active avors only (i.e. u,d,s). This implies that one has chosen $n_f = 3$ for the anomalous dimensions. In order to make this paper self-contained we give some details here. In LO where the input scale μ_0 is chosen to be $\mu_0^2 = \mu_{\text{LO}}^2 = 0.26$ ($\text{GeV} = c$)² the input parton densities are

$$\begin{aligned}
 xu_v(3;x; \mu_{\text{LO}}^2) &= 1.239 x^{0.48} (1 - x)^{2.72} (1 + 1.8 \frac{p}{\mu} \bar{x} + 9.5x) \\
 xd_v(3;x; \mu_{\text{LO}}^2) &= 0.614 (1 - x)^{0.9} xu_v(3;x; \mu_{\text{LO}}^2) \\
 x(3;x; \mu_{\text{LO}}^2) &= 0.23 x^{0.48} (1 - x)^{11.3} (1 + 12.0 \frac{p}{\mu} \bar{x} + 50.9x) \\
 x(u+d)(3;x; \mu_{\text{LO}}^2) &= 1.52 x^{0.15} (1 - x)^{9.1} (1 + 3.6 \frac{p}{\mu} \bar{x} + 7.8x) \\
 xg(3;x; \mu_{\text{LO}}^2) &= 17.47 x^{1.6} (1 - x)^{3.8} \\
 xs(3;x; \mu_{\text{LO}}^2) &= xs(x; \mu_{\text{LO}}^2) = 0
 \end{aligned} \tag{3.1}$$

In NLO where the input scale equals $\mu_{\text{NLO}}^2 = 0.40$ ($\text{GeV} = c$)² we have

$$\begin{aligned}
 xu_v(3;x; \mu_{\text{NLO}}^2) &= 0.632 x^{0.43} (1 - x)^{3.09} (1 + 18.2x) \\
 xd_v(3;x; \mu_{\text{NLO}}^2) &= 0.624 (1 - x)^{1.0} xu_v(3;x; \mu_{\text{NLO}}^2) \\
 x(3;x; \mu_{\text{NLO}}^2) &= 0.20 x^{0.43} (1 - x)^{12.4} (1 + 13.3 \frac{p}{\mu} \bar{x} + 60.0x) \\
 x(u+d)(3;x; \mu_{\text{NLO}}^2) &= 1.24 x^{0.20} (1 - x)^{8.5} (1 + 2.3 \frac{p}{\mu} \bar{x} + 5.7x) \\
 xg(3;x; \mu_{\text{NLO}}^2) &= 20.80 x^{1.6} (1 - x)^{4.1} \\
 xs(3;x; \mu_{\text{NLO}}^2) &= xs(x; \mu_{\text{NLO}}^2) = 0
 \end{aligned} \tag{3.2}$$

where $d = u$. Furthermore in [11] the heavy quark masses are $m_c = 1.4 \text{ GeV} = c^2$, $m_b = 4.5 \text{ GeV} = c$. In both sets the densities are evolved from a very low starting scale, where it is necessary to use the exact numerical solution for the running coupling constant $\alpha_s(m^2)$. The latter follows from the implicit equation

$$\ln \frac{Q^2}{\overline{m_s}^2} = \frac{4}{0} \alpha_s(m^2) - \frac{1}{2} \ln \frac{4}{0} \alpha_s(m^2) + \frac{1}{2} ;$$

$$_0 = 11 - \frac{2}{3} n_f ; \quad _1 = 102 - \frac{38}{3} n_f ; \quad (3.3)$$

and will be used in all the following formulae. Furthermore we adopt the values $\overline{m_s}^2_{3,4,5,6} = 299.4, 246, 167.7, 67.8 \text{ GeV}$ which yield $\alpha_s(5; M_Z^2) = 0.114$. Notice that the values for n_f follow from the matching conditions

$$\alpha_s(n_f; m^2) = \alpha_s(n_f + 1; m^2) ; \quad (3.4)$$

where for $n_f = 3$ and $n_f = 4$ one has to choose $m = m_c$ and $m = m_b$ respectively. For the computation of $F_{i;c}^{\text{EXACT}}$ (2.6) and $F_{i;c}^{\text{ASYMP}}$ (2.39) we take $n_f = 3$ for the parton densities and the running coupling constant in Eq. (3.3). However for $F_{i;c}^{\text{VFNS}}$ (2.29), $F_{i;c}^{\text{BMSN}}$ (2.39) and $F_{i;c}^{\text{PDF}}$ (2.40) we need $n_f = 4$ for the coupling constant in Eq. (3.3) and a parton density set with four active flavors (i.e. u, d, s, c) when the scale becomes larger or equal to the heavy flavor mass m . For reasons which will be explained below our computations are performed with parton densities represented in LO, NLO and NNLO (next-to-next-to leading order). The LO densities are convoluted with the order α_s^2 contributions to the coefficient functions. The NLO densities are convoluted with the order α_s parts of the coefficient functions. The zeroth order contributions to the latter have to be multiplied with the NNLO densities. Notice that for $n_f = 3$ we only need LO and NLO densities here since the heavy quark coefficient functions in $F_{i;c}^{\text{EXACT}}$ and $F_{i;c}^{\text{ASYMP}}$ start in order α_s . Our sets with four active flavors are derived from the ones with three active flavors by putting $n_f = 3$ in Eqs. (2.25)–(2.27) at a specific scale which we choose as $m^2 = m^2$. Hence it follows that in LO or in zeroth order α_s one gets

$$f_{k+k}^{\text{LO}}(4; x; m^2) = f_{k+k}^{\text{LO}}(3; x; m^2) ;$$

$$\begin{aligned}
f_{c+c}^{\text{LO}}(4; x; m^2) &= 0; \\
f_g^{\text{SLO}}(4; x; m^2) &= f_g^{\text{SLO}}(3; x; m^2); \tag{3.5}
\end{aligned}$$

whereas in NLO or in first order s one obtains

$$\begin{aligned}
f_{k+k}^{\text{NLO}}(4; x; m^2) &= f_{k+k}^{\text{NLO}}(3; x; m^2); \\
f_{c+c}^{\text{NLO}}(4; x; m^2) &= 0; \\
f_g^{\text{SNLO}}(4; x; m^2) &= f_g^{\text{SNLO}}(3; x; m^2); \tag{3.6}
\end{aligned}$$

Since the two-loop OME's $A_{qk}^{(2)}$, $A_{k1q}^{(2)}$ in Eqs. (2.25)–(2.27) do not vanish at $s^2 = m^2$ in the $\overline{\text{MS}}$ -scheme we find that in NNLO or in order s^2 the parton densities are discontinuous at $s^2 = m^2$ while going from three to four flavors i.e.

$$\begin{aligned}
f_{k+k}^{\text{NNLO}}(4; x; m^2) &\neq f_{k+k}^{\text{NNLO}}(3; x; m^2); \\
f_{c+c}^{\text{NNLO}}(4; x; m^2) &\neq 0; \\
f_g^{\text{SNNLO}}(4; x; m^2) &\neq f_g^{\text{SNNLO}}(3; x; m^2); \tag{3.7}
\end{aligned}$$

Note that if we would drop the terms independent of $\ln s^2/m^2$ in the operator matrix elements the inequalities in Eq. (3.7) would become equalities. Above $s = m_c$ all four flavor number densities evolve with $n_f = 4$ (we have not yet included a bottom quark density above $s = m_b$). The evolution of the parton densities, given by the renormalization group equations in Eq. (2.5), is determined by the anomalous dimensions $_{ij}^{(0)}$ (LO), $_{ij}^{(1)}$ (NLO) and $_{ij}^{(2)}$ (NNLO). Unfortunately the three-loop anomalous dimensions $_{ij}^{(2)}$ are not known yet except for the moments $N = 2; 4; 6; 8$ (see [19]). However an analysis of the light parton structure function in Eq. (2.1) [20] reveals that the contribution from $_{ij}^{(2)}$ is less important numerically than the contribution due to the two-loop coefficient functions computed in [12]. Hence our ignorance about the three-loop anomalous dimension will not appreciably alter our results. Therefore our NNLO analysis is only determined by the boundary conditions in Eq. (3.7) which only affects the charm density appearing in F_{ic}^{VFNS} , F_{ic}^{BMSN} and F_{ic}^{PDF} . The evolution of the parton densities

above $Q^2 = m_c^2$, presented in [21], was performed using a computer program which implements the direct x -space method (similar to that of [22]). The code is written in C++ and has the options to evolve densities in LO and NLO whereas the NNLO option presently only uses the NLO anomalous dimensions. We have checked that the evolution of the parton densities is in agreement with the results in [23].

Before substituting the parton densities into the structure functions we encounter a problem caused by the inequalities in Eq. (3.7). This happens in the threshold region which, according to the ACOT boundary conditions in Eq. (2.35), is defined by $Q^2 < m^2$. In this region one has to choose $Q^2 = m^2$ so that $F_{i;c}^{VFNS}(n_f = 4)$ and $F_{i;c}^{BM\,SN}(n_f = 4)$ are equal to $F_{i;c}^{EXACT}(n_f = 3)$. Notice that the latter has to be understood in the sense mentioned below Eq. (2.38) where $L_{i;k} \neq L_{i;k}^{HARD}$. However since $s(m^2)$ is rather large we have to truncate the perturbation series for the structure functions to the desired order otherwise the threshold behavior of all the $F_{i;c}^{VFNS}(n_f = 4)$ and $F_{i;c}^{BM\,SN}(n_f = 4)$ will be destroyed. Let us explain this for the BM SN scheme in Eq. (2.39). The arguments for the VFNS proceed in an analogous way. The conditions that the $F_{i;c}^{BM\,SN}(n_f = 4) = F_{i;c}^{EXACT}(n_f = 3)$ for $Q^2 = m^2$ implies that the $F_{i;c}^{ASYMP}(n_f = 3)$ in Eq. (2.39) are canceled by the $F_{i;c}^{PDF}(n_f = 4)$. Further we have to bear in mind that the $F_{i;c}^{EXACT}(n_f = 3)$ and $F_{i;c}^{ASYMP}(n_f = 3)$ are determined by the parton densities in the three flavor number scheme whereas the $F_{i;c}^{PDF}(n_f = 4)$ are constructed out of the four flavor number scheme parton densities. The latter have the form

$$\begin{aligned} f_k(4;x;m^2)^{NNLO} &= f_k(3;x;m^2)^{NNLO} [1 + O(\frac{2}{s})] \\ f_g^S(4;x;m^2)^{NNLO} &= f_g^S(3;x;m^2)^{NNLO} [1 + O(\frac{2}{s})] \\ C(4;x;m^2)^{NNLO} &= f_g^S(3;x;m^2)^{NNLO} O(\frac{2}{s}) + f_q^S(3;x;m^2)^{NNLO} O(\frac{2}{s}): \end{aligned} \quad (3.8)$$

If these densities are substituted in $F_{i;c}^{PDF}(n_f = 4)$ in Eq. (2.40) one obtains additional terms of order $\frac{3}{s}$ and $\frac{4}{s}$ in the perturbation series which are not canceled by $F_{i;c}^{ASYMP}(n_f = 3)$. Notice that the latter are only computed up to order $\frac{2}{s}$. This effect is caused by multiplying the four flavor number densities with the coefficient functions $C_{i;k}$ corrected beyond zeroth order in s . To avoid these higher order terms we propose the following formulae for

the structure functions in the VFN S

$$\begin{aligned}
F_{i,Q}^{\text{VFN S}}(n_f + 1; -Q^2; m^2) = & e_Q^2 f_{Q+Q}^{\text{NNLO}}(n_f + 1; -Q^2) C_{i,Q}^{\text{VFN SNS;}(0)}\left(\frac{Q^2}{m^2}\right) \\
& + a_s(n_f + 1; -Q^2) f_{Q+Q}^{\text{NLO}}(n_f + 1; -Q^2) C_{i,Q}^{\text{VFN SNS;}(1)}\left(\frac{Q^2}{m^2}; \frac{Q^2}{2}\right) \\
& + f_g^{\text{SNLO}}(n_f + 1; -Q^2) C_{i,Q}^{\text{VFN SNS;}(1)}\left(\frac{Q^2}{m^2}; \frac{Q^2}{2}\right) \\
& + a_s^2(n_f + 1; -Q^2) f_{Q+Q}^{\text{LO}}(n_f + 1; -Q^2) C_{i,Q}^{\text{VFN SNS;}(2)}(n_f + 1; \frac{Q^2}{m^2}; \frac{Q^2}{2}) \\
& + C_{i,Q}^{\text{VFN SPS;}(2)}\left(\frac{Q^2}{m^2}; \frac{Q^2}{2}\right) \sum_{k=1}^{X_f} f_{k+1}^{\text{LO}}(n_f + 1; -Q^2) C_{i,Q}^{\text{VFN SPS;}(2)}\left(\frac{Q^2}{m^2}; \frac{Q^2}{2}\right) \\
& + f_g^{\text{SLO}}(n_f + 1; -Q^2) C_{i,Q}^{\text{VFN SNS;}(2)}\left(\frac{Q^2}{m^2}; \frac{Q^2}{2}\right) \# \\
& + a_s^2(n_f + 1; -Q^2) \sum_{k=1}^{X_f} e_k^2 f_{k+1}^{\text{LO}}(n_f + 1; -Q^2) L_{i,Q}^{\text{HARD NS;}(2)}\left(\frac{Q^2}{m^2}\right) : \quad (3.9)
\end{aligned}$$

Notice that from the perturbative point of view the heavy quark density f_{Q+Q}^{LO} starts in order $a_s(-Q^2)$ so that after multiplication with $C_{i,Q}^{\text{VFN SNS;}(2)}$ and $C_{i,Q}^{\text{VFN SPS;}(2)}$ the product becomes of order $a_s^3(-Q^2)$. Hence these coefficient functions did not appear in the mass factorization relations (2.17)–(2.20) since the latter are carried out up to order $a_s^2(-Q^2)$. Since the heavy quark density in VFN S has to be treated on the same footing as the light flavor densities, in particular after resummation of the terms in $\ln^i(-Q^2/m^2)$, all densities are considered to start in zeroth order in perturbation theory. This explains the form of the above expression. Furthermore the coefficient functions $C_{i,Q}^{\text{VFN SNS;}(2)}$ and $C_{i,Q}^{\text{VFN SPS;}(2)}$ which originate from parton processes with an heavy quark in the initial state have not been calculated yet. Therefore we have to approximate them by the replacements

$$C_{i,Q}^{\text{VFN SNS;}(2)}(n_f + 1; \frac{Q^2}{m^2}; \frac{Q^2}{2}) \approx C_{i,Q}^{\text{NS;}(2)}(n_f + 1; \frac{Q^2}{2});$$

$$C_{i,Q}^{VFNS,PS;(2)} \frac{Q^2}{m^2}; \frac{Q^2}{2} \quad ! \quad C_{i,Q}^{VFNS,PS;(2)} \frac{Q^2}{m^2}; \frac{Q^2}{2} \quad ; \quad (3.10)$$

respectively. The remaining VFN S coefficient functions can be computed via the relations in Eqs. (2.17)–(2.20), which are defined in terms of the known H 's and A 's. The light partonic parts of the structure functions in the VFN S up to second order are given by

$$\begin{aligned} F_i^{VFNS,LIGHT} (n_f; ; Q^2) &= \sum_{k=1}^{X_f} e_k^2 f_{k+k}^{NNLO} (n_f + 1; ; Q^2) C_{i,g}^{NS;(0)} \\ &+ a_s (n_f + 1; ; Q^2) f_{k+k}^{NLO} (n_f + 1; ; Q^2) C_{i,g}^{NS;(1)} \left(\frac{Q^2}{2} \right) + f_g^{SNLO} (n_f + 1; ; Q^2) \\ &C_{i,g}^{S;(1)} \left(\frac{Q^2}{2} \right) + a_s^2 (n_f + 1; ; Q^2) f_{k+k}^{LO} (n_f + 1; ; Q^2) C_{i,g}^{NS;(2)} n_f; \frac{Q^2}{2} \\ &+ C_{i,g,Q}^{SOFTNS;(2)} ; \frac{Q^2}{m^2}; \frac{Q^2}{2} \sum_{l=1}^{X_f} f_{l+1}^{LO} (n_f + 1; ; Q^2) C_{i,g}^{PS;(2)} \frac{Q^2}{2} \\ &+ f_g^{SLO} (n_f + 1; ; Q^2) C_{i,g}^{S;(2)} \frac{Q^2}{2} ; \quad (3.11) \end{aligned}$$

with

$$\begin{aligned} C_{i,g,Q}^{SOFTNS;(2)} ; \frac{Q^2}{m^2}; \frac{Q^2}{2} &= L_{i,g,Q}^{SOFTNS;(2)} ; \frac{Q^2}{m^2} + F^{(2)} (Q^2; m^2) \\ &A_{qgQ}^{NS;(2)} \frac{2}{m^2} ! C_{i,g}^{NS;(0)} + \ln_0 \frac{2}{m^2} ! C_{i,g}^{NS;(1)} \frac{Q^2}{2} \quad (3.12) \end{aligned}$$

For the BM SN scheme we need the expression for $F_{i,Q}^{EXACT}$ as defined above Eq. (2.39)

$$\begin{aligned} F_{i,Q}^{EXACT} (n_f; ; Q^2; m^2) &= e_Q^2 a_s (n_f; ; Q^2) f_g^{SNLO} (n_f; ; Q^2) H_{i,g}^{S;(1)} \frac{Q^2}{m^2} \\ &+ a_s^2 (n_f; ; Q^2) \sum_{k=1}^{X_f} f_{k+k}^{LO} (n_f; ; Q^2) H_{i,g}^{PS;(2)} \frac{Q^2}{m^2}; \frac{Q^2}{2} \end{aligned}$$

$$\begin{aligned}
& + f_g^{S;LO} (n_f; \frac{Q^2}{m^2}) H_{ig}^{S;(2)} \frac{Q^2}{m^2} ; \frac{Q^2}{2})^{\#} \\
& + a_s^2 (n_f; \frac{Q^2}{m^2}) \sum_{k=1}^{X_f} e_k^2 f_{k+k}^{LO} (n_f; \frac{Q^2}{m^2}) L_{iq}^{HARD NS;(2)} ; \frac{Q^2}{m^2} : \quad (3.13)
\end{aligned}$$

If we choose the maximum $= s$ (defined in the figure caption for Fig. 5), we get $L_{iq}^{HARD NS;(2)} = 0$. On the other hand if the minimum value is adopted i.e. $= 4m^2$ one gets $L_{iq}^{HARD NS;(2)} = L_{iq}^{NS;(2)}$ and F_{iq}^{EXACT} becomes equal to the conventional expression given in Eq. (2.6). The structure function $F_{iq}^{ASYM P}$ is obtained from the expression above by replacing the exact coefficient functions by their asymptotic analogues. Furthermore to calculate F_{iq}^{BMSN} in Eq. (2.39) we need

$$\begin{aligned}
F_{iq}^{PDF} (n_f + 1; \frac{Q^2}{m^2}) &= e_Q^2 f_{Q+Q}^{NNLO} (n_f + 1; \frac{Q^2}{m^2}) C_{iq}^{NS;(0)} \\
& + a_s (n_f + 1; \frac{Q^2}{m^2}) f_{Q+Q}^{NLO} (n_f + 1; \frac{Q^2}{m^2}) C_{iq}^{NS;(1)} (\frac{Q^2}{2}) \\
& + f_g^{SNLO} (n_f + 1; \frac{Q^2}{m^2}) C_{ig}^{S;(1)} (\frac{Q^2}{2}) \\
& + a_s^2 (n_f + 1; \frac{Q^2}{m^2}) f_{Q+Q}^{LO} (n_f + 1; \frac{Q^2}{m^2}) C_{iq}^{NS;(2)} (n_f + 1; \frac{Q^2}{2}) \\
& + C_{iq}^{PS;(2)} \frac{Q^2}{2} ! + \sum_{l=1}^{X_f} f_{l+1}^{LO} (n_f + 1; \frac{Q^2}{m^2}) C_{iq}^{PS;(2)} \frac{Q^2}{2} \\
& + f_g^{S;LO} (n_f + 1; \frac{Q^2}{m^2}) C_{ig}^{S;(2)} (\frac{Q^2}{2})^{\#} \\
& + a_s^2 (n_f + 1; \frac{Q^2}{m^2}) \sum_{k=1}^{X_f} e_k^2 f_{k+k}^{LO} (n_f; \frac{Q^2}{m^2}) L_{iq}^{HARD ASYMP NS;(2)} ; \frac{Q^2}{m^2} : \quad (3.14)
\end{aligned}$$

Finally up to order $\frac{2}{s}$, Eq. (2.41) becomes

$$\begin{aligned}
 F_i^{\text{BM SN LGHT}}(n_f + 1; \frac{Q^2}{s}) &= \sum_{k=1}^{N_f} e_k^2 f_{k+k}^{\text{NNLO}}(n_f + 1; \frac{Q^2}{s}) C_{i;q}^{\text{NS};(0)} \\
 &+ a_s(n_f + 1; \frac{Q^2}{s}) f_{k+k}^{\text{NLO}}(n_f + 1; \frac{Q^2}{s}) C_{i;q}^{\text{NS};(1)}(\frac{Q^2}{s}) + f_g^{\text{SNLO}}(n_f + 1; \frac{Q^2}{s}) \\
 &C_{i;q}^{\text{S};(1)}(\frac{Q^2}{s}) + a_s^2(n_f + 1; \frac{Q^2}{s}) f_{k+k}^{\text{LO}}(n_f + 1; \frac{Q^2}{s}) C_{i;q}^{\text{NS};(2)}(\frac{Q^2}{s}) \\
 &+ \sum_{l=1}^{N_f} f_{l+1}^{\text{LO}}(n_f + 1; \frac{Q^2}{s}) C_{i;q}^{\text{PS};(2)}(\frac{Q^2}{s}) + f_g^{\text{SLO}}(n_f + 1; \frac{Q^2}{s}) C_{i;q}^{\text{S};(2)}(\frac{Q^2}{s}) \\
 &+ a_s^2(n_f + 1; \frac{Q^2}{s}) \sum_{k=1}^{N_f} e_k^2 f_{k+k}^{\text{LO}}(n_f; \frac{Q^2}{s}) L_{i;q}^{\text{SOFT NS};(2)}(\frac{Q^2}{s}; \frac{m^2}{s}) \\
 &L_{i;q}^{\text{ASYMP NS};(2)}(\frac{Q^2}{s}) + F^{(2)}(Q^2; m^2) F^{\text{ASYMP};(2)}(Q^2; m^2) C_{i;q}^{\text{NS};(0)} : \\
 \end{aligned} \tag{3.15}$$

Notice that we have the relations

$$C_{i;q}^{\text{NS};(2)}(n_f + 1; \frac{Q^2}{s}) = C_{i;q}^{\text{NS};(2)}(n_f; \frac{Q^2}{s}) + C_{i;q;Q}^{\text{NS};(2)}(\frac{Q^2}{s}); \tag{3.16}$$

with

$$\begin{aligned}
 C_{i;q;Q}^{\text{NS};(2)}(\frac{Q^2}{s}) &= L_{i;q}^{\text{ASYMP NS};(2)}(\frac{Q^2}{s}) + F^{\text{ASYMP};(2)}(Q^2; m^2) \\
 A_{q;q;Q}^{\text{NS};(2)}(\frac{2}{m^2}) C_{i;q}^{\text{NS};(0)} &+ \alpha_Q \ln(\frac{2}{m^2}) C_{i;q}^{\text{NS};(1)}(\frac{Q^2}{s}) : \tag{3.17}
 \end{aligned}$$

The first and second terms in the expression above cancel the third last and final term in Eq. (3.15). The result is then equal to $C_{i;q;Q}^{\text{SOFT NS};(2)}$ in Eq. (3.11) in the limit $Q^2 \gg m^2$. The form of the above structure functions also suppresses higher order terms beyond $\frac{2}{s}$ arising from the three flavor

number parton densities since the latter also contain term s proportional to s and higher. This becomes apparent if one takes the N th moments of the densities. For instance we observe the following behavior up to NNLO in the non-singlet case

$$\begin{aligned}
 f_q^{LO;N}(s) &= \frac{s(\frac{2}{0})}{s(\frac{2}{0})} f_q^{LO;N}(s) \\
 f_q^{NLO;N}(s) &= \frac{h}{1 + s(\frac{2}{0}) A_q^{(1)}} \frac{s(\frac{2}{0})}{s(\frac{2}{0})} f_q^{NLO;N}(s) \\
 f_q^{NNLO;N}(s) &= \frac{h}{1 + s(\frac{2}{0}) A_q^{(1)} + \frac{2}{s} s(\frac{2}{0}) A_q^{(2)}} \frac{s(\frac{2}{0})}{s(\frac{2}{0})} f_q^{NNLO;N}(s) \\
 f_q^{NNLO;N}(s) &:
 \end{aligned} \tag{3.18}$$

The choice of the multiplication rules above avoids the appearance of scheme dependent terms beyond the order in which we want to compute the structure functions. The above prescription guarantees that for $Q^2 < m^2$ we satisfy the condition $F_{i;c} = F_{i;c}^{\text{EXACT}}(n_f)$ in both schemes.

In the subsequent part of this section we will only discuss the case where the heavy quark is the charm quark, i.e. $Q = c$. Hence in all expressions above we have to choose $n_f = 3$. Further we have to make a choice for the cut ϵ appearing in the coefficient functions $L_{k;q}^{\text{SOFTNS};(2)}$ ($k = 2; L$). The $\epsilon = (s - 4m^2)/(s + 4m^2)$ dependence of $xL_{2;q}^{\text{SOFTNS};(2)}$ is shown in Fig. 8, where one notes that it peaks at large x , i.e., near threshold. (The plot for $xL_{L;q}^{\text{SOFTNS};(2)}$ has a similar shape). After convoluting this function with the parton densities its contribution to the structure function F_2^{LIGHT} only amounts to a few percent at $Q^2 = 10^3$ (GeV=c)². At decreasing Q^2 the contribution becomes even smaller. The same holds for $L_{2;q}^{\text{HARD}}$ contributing to $F_{2;c}$. Hence the dependence of the structure functions on the value of ϵ will be very small. Therefore in the subsequent analysis we choose $\epsilon = s$ which implies that $L_{i;q}^{\text{HARD}}$ contribution vanishes and the $L_{i;q}^{\text{SOFT}}$ part attains its maximum. Other choices hardly affect the plots so that our conclusions will be unaltered.

Next we present the x -dependence of the NNLO charm density (see Eq. (3.7)) for various values of Q^2 in Figs. 9a,b. The latter plot emphasizes the

region $0.01 < x < 1$. At $\tau = m^2$ it becomes negative for $x < 0.007$ which is due to the boundary condition in Eq. (2.23) and the momentum sum rule. When $\tau > m^2$ the density becomes positive over the whole x range. In Figs. 9c and 9d we have shown the charm densities in NLO which are obtained from [17] and [18] respectively, with an offset scale so that they can easily be compared with Fig. 9a. The former is constructed in the TR scheme whereas the latter follows the prescription of ACO T. Both are positive over the whole x range. Our LO and NLO parameterizations, which are not shown in the figures, are also positive for all values of x . This property can be traced back to the boundary conditions which yield in LO and NLO $c(x; m^2) = 0$. Note that a direct comparison between the charm densities from different groups is not meaningful because each group fits different data to determine their respective input three flavor number gluon densities. However it seems that our charm density, at small τ^2 , does not rise as steeply as that of the CTEQ 5HQ [18] at small x . It is more similar to the MSTW98 (central gluon) [17] density. In Fig. 10 we make a comparison between our charm density which evolves according to the renormalization group equation and the one computed in fixed order perturbation theory (FOPT) via Eq. (2.23). To that order we have plotted

$$R(x; \tau^2) = \frac{c^{\text{EVOLVED}}(x; \tau^2)}{c^{\text{FOPT}}(x; \tau^2)} : \quad (3.19)$$

The density c^{FOPT} is computed up to order τ^2 since the OME's in Eq. (2.26) are only known up to that order. In Fig. 10a we have shown the ratio in LO. The latter implies that we have only kept the leading logarithms in $\ln \tau^2/m^2$ in the OME's which are resummed in all orders in c^{EVOLVED} . The deviation of R from unity shows the effect of the resummation. The same ratio is shown in NLO in Fig. 10b where we also included the subleading terms in the OME's. Finally if we take into account the non-logarithmic terms in the two-loop OME's $A_{Qg}^{S;(2)}$ and $A_{Qq}^{PS;(2)}$ (2.26) one obtains the NNLO ratio (see Fig. 10c). The figures reveal that in LO and NLO the effect of the resummation is very small except near $x = 1$. This picture changes if we go to NNLO where the deviation of R from one becomes appreciable when x tends to zero. Here R can even become negative which happens for $\tau^2 < 3$ (GeV = c^2). This effect is wholly due to the boundary condition $c(x; m^2) \neq 0$ which occurs beyond NLO. Furthermore the figures reveal that $R > 1$ at large x whereas $R < 1$ at small x . Notice that in Fig. 10c $c^{\text{FOPT}}(x; \tau^2) = 0$ for $x = 0.007$

at $2 = 2$ ($\text{GeV} = c$)² so that $R = 1$ which explains the bump in the figure. Figure 10c is important because it shows that $C^{\text{EVOLVED}}(x; Q^2) < C^{\text{OPT}}(x; Q^2)$ at small x . The consequence is that $F_{1;c}^{\text{BM SN}}(x; Q^2)$ and $F_{1;c}^{\text{VFNS}}(x; Q^2)$ will become smaller than $F_{1;c}^{\text{EXACT}}(x; Q^2)$ when Q^2 becomes slightly larger than m_c^2 due to the choice made for the factorization scale in Eq. (2.35). This can even lead to a negative structure function as will happen for $F_{L;c}^{\text{VFNS}}$ which we will see later on.

Now we present results for the various structure functions. In Fig. 11 we show the charm quark structure functions in NNLO given by $F_{2;c}^{\text{VFNS}}(n_f = 4)$, $F_{2;c}^{\text{BM SN}}(n_f = 4)$, $F_{2;c}^{\text{PDF}}(n_f = 4)$ and $F_{2;c}^{\text{EXACT}}(n_f = 3)$ plotted in the region $1 < Q^2 < 10^3$ ($\text{GeV} = c$)² for $x = 0.05$. The figure reveals that there is hardly any difference between the BM SN and VFNS prescriptions. The curves in both prescriptions lie between the ones representing $F_{2;c}^{\text{PDF}}(n_f = 4)$ and $F_{2;c}^{\text{EXACT}}(n_f = 3)$ except for low Q^2 . In this region the latter is a little bit larger than the other ones which is expected from the discussion of the charm density given above. Notice that in the low Q^2 region $F_{2;c}^{\text{PDF}}(n_f = 4)$ becomes negative which means that charm quark electroproduction cannot be described by this quantity anymore. In Fig. 12 we present the same plots for $x = 0.005$. Again one cannot distinguish between $F_{2;c}^{\text{BM SN}}(n_f = 4)$ and $F_{2;c}^{\text{VFNS}}(n_f = 4)$ but now both are smaller than $F_{2;c}^{\text{EXACT}}(n_f = 3)$ over the whole Q^2 range. The latter is even larger than $F_{2;c}^{\text{PDF}}(n_f = 4)$ in particular for $Q^2 > 50$ ($\text{GeV} = c$)². Further we want to emphasize that due to our careful treatment of the threshold region there is an excellent cancellation (to three significant places) between $F_{2;c}^{\text{PDF}}(n_f = 4)$ and $F_{2;c}^{\text{ASYMP}}(n_f = 3)$ at very small Q^2 so that both $F_{2;c}^{\text{VFNS}}(n_f = 4)$ and $F_{2;c}^{\text{BM SN}}(n_f = 4)$ tend to $F_{2;c}^{\text{EXACT}}(n_f = 3)$. Also at large Q^2 we have an excellent cancellation between $F_{2;c}^{\text{ASYMP}}(n_f = 3)$ and $F_{2;c}^{\text{EXACT}}(n_f = 3)$ so that both $F_{2;c}^{\text{VFNS}}(n_f = 4)$ and $F_{2;c}^{\text{BM SN}}(n_f = 4)$ tend to $F_{2;c}^{\text{PDF}}(n_f = 4)$ (see Eq. (2.44)).

In Fig. 13 we show similar plots as in Fig. 11 but now for the charm quark longitudinal structure functions. Here we observe a difference between the plots for $F_{L;c}^{\text{VFNS}}(n_f = 4)$ and $F_{L;c}^{\text{BM SN}}(n_f = 4)$ in the region $m_c^2 < Q^2 < 40$ ($\text{GeV} = c$)². In particular the latter tends to $F_{L;c}^{\text{EXACT}}(n_f = 3)$ while the former is larger. Furthermore $F_{L;c}^{\text{PDF}}(n_f = 3)$ is considerably larger than the other three structure functions, which differs from the behavior seen in Fig. 11. This can be mainly attributed to the gluon density which plays a more prominent role in $F_{L;c}$ than in $F_{2;c}$. For $x = 0.005$ (see Fig. 14) the difference between the BM SN and the VFNS descriptions becomes even

more conspicuous. In this case $F_{L;c}^{VFNS}(n_f = 4)$ becomes negative in the region $m_c^2 < Q^2 < 7$ ($GeV = c$)² which is unphysical. This effect can be attributed to the zeroth order longitudinal coefficient function in Eq. (3.9), which behaves like $C_{L,Q}^{VFNS,NS;(0)} = 4m^2 = Q^2$ (see [15]), and the non-vanishing charm density at $Q^2 = m_c^2$. In the case of BM SN the longitudinal coefficient function is equal to zero in lowest order so that $F_{L;c}^{BM SN}(n_f = 4)$ does not become negative.

In Figs. 15 and 16 we make a comparison between the NLO and the NNLO structure functions $F_{2;c}^{VFNS}(n_f = 4)$ and $F_{2;c}^{BM SN}(n_f = 4)$. Both prescriptions i.e. VFNS and BM SN lead to the same result in NNLO. However while going from NLO to NNLO the structure function $F_{2;c}^{VFNS}(n_f = 4)$ decreases whereas $F_{2;c}^{BM SN}(n_f = 4)$ increases a little bit. The differences in the case of $x = 0.005$ are even smaller than those observed for $x = 0.05$. The same comparison between NLO and NNLO is made for the longitudinal structure functions in Figs. 17 and 18. Here the differences between NLO and NNLO are much larger than in the case of $F_{2;c}$ in Figs. 15,16. In NLO $F_{L;c}^{BM SN}(n_f = 4)$ is smaller than the one plotted for NNLO. However for $F_{L;c}^{VFNS}(n_f = 4)$ we see a decrease in the small Q^2 -region while going from NLO to NNLO whereas for large Q^2 we observe the opposite. In particular the valley in the region $m_c^2 < Q^2 < 7$ ($GeV = c$)² observed for $F_{L;c}^{VFNS}(n_f = 4)$ at $x = 0.005$ in NNLO turns into a bump. This is due to the boundary condition on the charm density which in NLO vanishes at $Q^2 = m_c^2$ whereas in NNLO it is negative at small x -values (see Fig. 10c). From the observations above one can conclude that the VFNS prescription bedevils the threshold (low Q^2) behavior for $F_{L;c}$ due to the non-vanishing zeroth order longitudinal coefficient function $C_{L,Q}^{VFNS,NS;(0)}$. This problem is avoided by TR in [10] by imposing a condition on the structure functions as indicated in Eq. (2.36). Hence our results for $F_{i;c}^{BM SN}$ agree reasonably well for $i = 2$ and $i = L$ with those presented in NLO by TR in [10]. This is mainly due to the fact that there is only a small difference between the NLO and NNLO approximations in the BM SN scheme. It also reveals that the condition in Eq. (2.36) for $i = L$ can be mimicked by a vanishing zeroth order longitudinal coefficient function. Note that results for the x -values presented above are representative for the whole range $5 \cdot 10^{-5} < x < 0.5$.

To summarize the main points of this paper we have discussed two variable flavor number schemes for charm quark electroproduction in NNLO. They are distinguished by the way mass factorization is implemented. In

the VFNS this is done with respect to the full heavy and light quark structure functions at finite Q^2 . In the BM SN scheme the mass factorization is only applied to the coefficient functions in the large Q^2 limit. Both schemes require three flavor and four flavor number parton densities which satisfy NNLO matching conditions at a scale $Q^2 = m^2$. We have constructed these densities using our own evolution code. The schemes also require matching conditions on the coefficient functions which are implemented in this paper. We have also made a careful analysis of the remnant of dangerous terms in $\ln(Q^2/m^2)$ from the Compton contributions so that both $F_{i;c}^{\text{VFNS}}(n_f + 1)$ and $F_{i;c}^{\text{BM SN}}(n_f + 1)$ are collinear safe. We have done this in a way which is simplest from the theoretical point of view, by implementing a cut on the mass of the cc pair. We have not attempted to make any comparison with experimental data. This we postpone to a later date as it requires a variable flavor number scheme description of differential distributions. However we stress that any charm quark density description of $F_{i;c}$ must use collinear safe definitions. This is not required in the fixed order perturbation theory approach given by $F_{i;c}^{\text{EXACT}}$ in [5] for moderate Q^2 -values.

Finally we made a careful analysis of the threshold behaviors of $F_{i;c}^{\text{VFNS}}(n_f + 1)$ and $F_{i;c}^{\text{BM SN}}(n_f + 1)$. In order to achieve the required cancellations near threshold so that they both become equal to $F_{i;c}^{\text{EXACT}}(n_f)$ one must be very careful to combine terms with the same order in the expansion in the running coupling constant α_s . Therefore technically we require six sets of parton densities, namely the LO, NLO and NNLO three flavor number sets and the LO, NLO and NNLO four flavor number sets. However not all the necessary theoretical inputs are available to us to finish this task. The approximations we made in this paper were sufficient to provide very clear answers. We successfully implemented the required cancellations near threshold and the corresponding limits at large scales came out naturally. Inconsistent sets of parton densities automatically spoil these cancellations. We did not have to use matching conditions on derivatives of structure functions as proposed in [10], which seem very artificial. The numerical results do however end up quite similar. We have also shown that the VFNS defined above leads to an unnatural behavior of the longitudinal structure function in the threshold region which is due to a non-vanishing zeroth order coefficient function. Since there are no other differences between the VFNS and BM SN schemes we recommend the latter because it is less complicated than the former. In particular it does not need additional coefficient functions other than the

existing heavy quark and light parton coefficient functions available in the literature.

ACKNOWLEDGMENTS

The work of A. Chuvakin and J. Smith was partially supported by the National Science Foundation grant PHY-9722101. The work of W. L. van Neerven was supported by the EC network 'QCD and Particle Structure' under contract No. FMRX-CT-98-0194.

Appendix A

In this appendix we present the exact expressions for the heavy quark coefficient functions $L_{i,q}^{(2)}$ corresponding to the Compton process in Fig. 5 when there is a cut on the invariant mass s_{QQ} of the heavy quark pair. As explained in [14] the calculation is straightforward because one can first integrate over the heavy quark momenta in the final state without affecting the momentum of the remaining light quark. The phase space integrals are the same as the ones obtained for the process $(q) + q(k_1) \rightarrow g + q(g \rightarrow Q + \bar{Q})$ where the gluon becomes virtual. In the expressions for the complete integration over the virtual mass s_{QQ} of the gluon (see Fig. 5) one integrates over the range $4m^2 \leq s_{QQ} \leq s$ with $s = (q+k_1)^2$. The resulting expressions, called $L_{i,q}^{r,(2)}$ with $r = NS; S$ and $i = 2; L$ are presented in appendix A of [14]. Notice that up to order $\frac{2}{s}$ there is no difference between singlet and non-singlet so that $L_{i,q}^{NS,(2)} = L_{i,q}^{S,(2)}$. If we limit the range of integration to $4m^2 \leq s_{QQ} \leq s$ one obtains

$$\begin{aligned}
L_{L,q}^{\text{SOFT,NS},(2)}(z; \frac{Q^2}{m^2}) = & C_F T_f \sum_i^n 96a^2(s) z (1-z)^2 \overset{h}{L}_1 (L_2 + L_4 + L_5) \\
& 2(D \text{IL}_1 - D \text{IL}_2 - D \text{IL}_3 + D \text{IL}_4) - 32\tilde{a}^2(s) \text{IL} + 3(1-z) \\
& 6(1-z)^2 \text{IL}_1 + \frac{16}{3}z \overset{h}{L}_1 - 26a(s)(1-z) + 88\tilde{a}(s)(1-z)^2 \frac{i \text{L}_3}{s \text{Q}} \\
& \frac{256}{3}b(\text{a})(s)z(1-z)(1-d(\text{a})) \overset{h}{L}_6 + \frac{64}{3}b(\text{a})(s) \overset{h}{L}_2 + 10(1-z) \\
& 14(1-z)^2 d(\text{a}) \overset{h}{L}_2 - (1-z) \overset{h}{L}_3 (1-z)^2 \\
& 128b(\text{a})d(\text{a})^2(s)z(1-z)^2 (1+2d(\text{a})) \overset{h}{L}_6 \\
& + \frac{64}{3}b(\text{a})d(\text{a})^2(s) \overset{h}{L}_1 + 2d(\text{a}) \overset{h}{L}_1 + 3(1-z) \overset{h}{L}_6 (1-z)^2 \\
& \frac{32}{3}b(\text{a})z + \frac{16}{9}b^3(\text{a})z; \tag{A.1}
\end{aligned}$$

$$\begin{aligned}
L_{2,q}^{\text{SOFT,NS},(2)}(z; \frac{Q^2}{m^2}) = & C_F T_f \left(\frac{4}{3} \frac{1+z^2}{1-z} - 16\tilde{a}^2(s)(1-z) \text{IL} \right. \\
& \left. 9(1-z) + 9(1-z) \text{IL}_1 (L_2 + L_4 + L_5) - 2(D \text{IL}_1 - D \text{IL}_2) \right)
\end{aligned}$$

$$\begin{aligned}
& D \text{ IL}_3 + D \text{ IL}_4) \left[\frac{8}{3} - \frac{4}{1-z} + 8a^2(s) \mathcal{L} + 18(1-z) \right. \\
& \left. 36(1-z^2) + \frac{1}{1-z} \right] L_1 + \frac{8}{9} [28 - 17(1-z) - \frac{19}{1-z}] \\
& + \frac{16}{9} a(s) [61 - 160(1-z) + 128(1-z^2)] \\
& - \frac{64}{9} a^2(s) (1-z) [23 - 104(1-z) + 94(1-z^2)] \frac{L_3}{sq_2} \\
& + \frac{64}{3} b(\) a(s) \frac{h}{2} - 7(1-z) + 6(1-z^2)(1-d(\)) \\
& + d(\) a(s) (1-z) [1 - 9(1-z) + 9(1-z^2)] (1 + 2d(\)) \frac{i}{L_6} \\
& + \frac{8}{9} b(\) 6 - b(\) \frac{h}{2} - (1-z) \frac{2}{1-z} \frac{i}{L_6} \\
& - \frac{32}{3} b(\) d(\) a(s) \frac{h}{7} - 3(1-z) - 9(1-z^2) \frac{1}{1-z} \frac{i}{z} \\
& - \frac{32}{9} b(\) a(s) \frac{h}{2} - 95(1-z) + 121(1-z^2) + \frac{3}{1-z} \frac{i}{z} \\
& + \frac{16}{3} b(\) d(\) a^2(s) 1 + 2d(\) \frac{h}{2} + 18(1-z) \\
& - 36(1-z^2) + \frac{1}{1-z} \frac{i}{z} - \frac{8}{9} b(\) \frac{h}{50} - 34(1-z) \frac{29}{1-z} \frac{i}{z} \\
& + \frac{4}{27} b^3(\) 38 - 28(1-z) \frac{17}{1-z} \frac{i}{z} ; \quad (A.2)
\end{aligned}$$

where the partonic scaling variable is equal to $z = Q^2/(2q_1) = Q^2/(s+Q^2)$,
Further we have defined

$$\begin{aligned}
& s \frac{z}{(1-z)} ; \quad s \frac{z}{1-\frac{4}{z}} ; \quad s \frac{z}{1-\frac{4}{z}} ; \\
& a(s) = \frac{m^2}{s} = \frac{z}{(1-z)} ; \quad b(\) = \frac{m^2}{1-\frac{4}{z}} ; \quad d(\) = \frac{z}{4m^2} ; \\
& L_1 = \ln \frac{1+b(\)}{1-b(\)} ; \quad L_2 = \ln \frac{1+sq_2}{1-sq_2} ; \quad L_3 = \ln \frac{sq_2+b(\)}{sq_2-b(\)} ; \\
& L_4 = \ln \frac{1}{z^2} ; \quad L_5 = \ln \frac{1}{1-sq_1^2} ; \quad L_6 = \ln \frac{sq_2^2-b(\)}{z(1-sq_1^2)} ; \\
& D \text{ IL}_1 = L_2 \frac{(1-sq_2^2)(1+b(\))}{(1+sq_2)(1-b(\))} ; \quad D \text{ IL}_2 = L_2 \frac{1}{1+b(\)} ;
\end{aligned}$$

$$D \text{IL}_3 = L_{i2} \frac{1 - b(\beta)}{1 + s_{Q2}} \quad ; \quad D \text{IL}_4 = L_{i2} \frac{1 + b(\beta)}{1 + s_{Q2}} : \quad (\text{A.3})$$

The variable β , which allows us to distinguish between soft and hard (observable) heavy quark anti-quark pairs, is in the range $4m^2 \leq \beta \leq s$. The variable z is in the range $0 \leq z \leq (s + 4m^2)/s$.

Note that when $\beta = s$ one obtains $L_{i2}^{\text{SOFT NS};(2)}$! $L_{i2}^{\text{NS};(2)}$ which are reported in [14]. When the integration range is given by $s_{Q2} \leq \beta \leq s$ we get $L_{i2}^{\text{HARD NS};(2)}$ which are given by

$$L_{i2}^{\text{HARD NS};(2)}(z; \beta; \frac{Q^2}{m^2}) = L_{i2}^{\text{NS};(2)}(z; \frac{Q^2}{m^2}) - L_{i2}^{\text{SOFT NS};(2)}(z; \beta; \frac{Q^2}{m^2}) : \quad (\text{A.4})$$

Notice that $L_{i2}^{\text{HARD NS};(2)}$ is finite in the limit $\beta \rightarrow 0$ so that it does not contain collinear divergences. The latter can be wholly attributed to $L_{i2}^{\text{SOFT NS};(2)}$ as is revealed if one takes the limit $Q^2 \rightarrow 1$. In this case the expressions (A.1) and (A.2) reduce to

$$\begin{aligned} L_{i2}^{\text{SOFT ASYMP NS};(2)}(z; \beta; \frac{Q^2}{m^2}) = & C_F T_f \left[\frac{16}{3} z \ln \frac{Q^2}{m^2} - \frac{16}{3} z \ln \frac{Q^2}{m^2} \right] z \\ & + \frac{32}{3} z \ln \frac{1 + b(\beta)}{2} - \frac{80}{9} z - \frac{80}{9} (b(\beta) - 1) z + \frac{16}{9} b(\beta) b^2(\beta) - 1 z \\ & + b(\beta) \left[\frac{64}{3} \frac{Q^2}{Q^2} z^2 - \frac{16}{Q^4} z^3 \ln^h \frac{Q^2}{m^2} - z \frac{(1 - z)^h}{z^2} \right] \\ & \left. \frac{16}{3} \frac{Q^2}{Q^2} z \frac{2}{1 - z} \right] 4 + 3z + \frac{8}{3} \frac{Q^2}{Q^4} z^2 \frac{1}{(1 - z)^h} + \frac{3}{1 - z} \quad \# \quad (\text{A.5}) \end{aligned}$$

and

$$\begin{aligned} L_{2i2}^{\text{SOFT ASYMP NS};(2)}(z; \beta; \frac{Q^2}{m^2}) = & C_F T_f \left[\frac{1 + z^2}{1 - z} \right] \left[\frac{8}{3} \ln \frac{Q^2}{m^2} \ln \frac{1}{z^2} z \right. \\ & + \frac{8}{3} \ln \frac{Q^2}{m^2} + \frac{16}{3} \ln \frac{1}{z^2} z + \frac{8}{3} \ln \frac{Q^2}{m^2} - \frac{116}{9} \ln \frac{1 + b(\beta)}{2} \\ & + \frac{4}{3} \ln^2 \frac{Q^2}{m^2} - \frac{4}{3} \ln^2 \frac{Q^2}{m^2} - \frac{8}{3} \ln \frac{Q^2}{m^2} \ln \frac{1}{z^2} z - \frac{8}{3} L_{i2} \frac{z(1 + b(\beta))}{2Q^2} \\ & \left. \frac{8}{3} L_{i2} \frac{1 + b(\beta)}{2} + \frac{8}{3} L_{i2} \frac{2m^2}{(1 + b(\beta))} \right] \frac{58}{9} \ln \frac{Q^2}{m^2} - 2 \ln \frac{Q^2}{m^2} \end{aligned}$$

$$\begin{aligned}
& + 4 \ln \frac{Q^2}{z} - z - \frac{40}{9} \ln \frac{1}{z^2} z + \frac{314}{27} + \frac{2}{3} + \frac{26}{3} z \ln \frac{Q^2}{m^2} \\
& + \frac{2}{3} 2z \ln \frac{Q^2}{z} - \frac{4}{3} + \frac{20}{3} z \ln \left(\frac{Q^2}{z} - z \right) + \frac{4}{3} + \frac{52}{3} z \ln \frac{1 + b(\)}{2} \\
& \frac{10}{9} \frac{130}{9} z + b(\) \ln \frac{16}{3 Q^2} z \frac{2}{1 - z} - 1 - 6z + \frac{8}{3 Q^4} z^2 \frac{1}{1 - z} \\
& 9z \ln \frac{Q^2}{z} - z \frac{(1 - z)^i}{z^2} - \frac{8}{3 Q^2} z \frac{7}{1 - z} - 12 + 9z \frac{1}{(1 - z)^2} \\
& + \frac{2}{3 Q^4} z^2 \frac{2}{(1 - z)^2} + \frac{18}{1 - z} - 36 + \frac{1}{(1 - z)^3} + \frac{8}{9} b(\) (1 - b^2(\)) \\
& + \frac{40}{9} b(\) - 1 - 1 + z \frac{2}{1 - z} \ln \frac{Q^2}{z} - z \frac{(1 - z)^i}{z^2} \\
& + \frac{4}{27} b(\) b^2(\) - 1 - 10 + 28z \frac{17}{1 - z} + (b(\) - 1) \frac{344}{27} \\
& \frac{704}{27} z + \frac{628}{27} \frac{1}{1 - z} \tag{A.6}
\end{aligned}$$

respectively. In the limit $m \rightarrow 0$ the results above show the same logarithmic terms in $\ln^i(Q^2/m^2)$ ($i = 1, 2$) as the asymptotic expressions for $L_{1,q}^{r,(2)}$ given in Eqs. (D.7) and (D.8) of [14]. Hence the differences between the results there and the asymptotic expressions above are free of any terms in $\ln(Q^2/m^2)$. The asymptotic expressions of $L_{1,q}^{\text{HARD}, r,(2)}$ for $Q^2 \rightarrow 1$ are given by

$$\begin{aligned}
L_{1,q}^{\text{HARD, ASYMPS}, (2)}(z; \frac{Q^2}{m^2}) &= C_F T_F \frac{16}{3} z \ln \frac{1}{z^2} z + \frac{16}{3} z \ln \frac{Q^2}{z} - z \\
& + \frac{32}{3} z \ln \frac{1 + b(\)}{2} + \frac{16}{3} - \frac{40}{3} z + \frac{80}{9} (b(\) - 1) z + \frac{16}{9} b(\) - 1 \\
& b(\) z - b(\) \frac{64}{3 Q^2} z^2 - \frac{16}{Q^4} z^3 \ln \frac{Q^2}{z} - z \frac{(1 - z)^i}{z^2} \\
& + \frac{16}{3 Q^2} z \frac{2}{1 - z} - 4 + 3z + \frac{8}{3 Q^4} z^2 \frac{1}{(1 - z)^2} + \frac{3}{1 - z} - 6 \quad ; \\
& \tag{A.7}
\end{aligned}$$

and

$$L_{2,q}^{\text{HARD, ASYMPS}, (2)}(z; \frac{Q^2}{m^2}) = C_F T_F \frac{1 + z^2}{1 - z} - \frac{4}{3} \ln^2(1 - z)$$

$$\begin{aligned}
& 2 \ln \frac{1}{z^2} z - \frac{16}{3} \ln z \ln(1-z) + 6 \ln z + \frac{5}{3} + \frac{4}{3} \ln^2 \frac{Q^2}{z^2} \\
& + \frac{8}{3} \ln \frac{Q^2}{z^2} \ln \frac{1}{z^2} z + \frac{116}{9} - \frac{8}{3} \ln \frac{Q^2}{m^2} - \frac{16}{3} \ln \frac{1}{z^2} z - \frac{8}{3} \ln \frac{Q^2}{z^2} \\
& \ln \frac{1+b(\))}{2} + \frac{8}{3} \text{Li}_2 \frac{z(1+b(\))}{2Q^2} + \frac{8}{3} \text{Li}_2 \frac{1+b(\))}{2} - \frac{8}{3} \\
& \frac{8}{3} \text{Li}_2(1-z) - \frac{8}{3} \text{Li}_2 \frac{2m^2}{(1+b(\))} + 2 \ln \frac{Q^2}{z} - 4 \ln \frac{Q^2}{z} \\
& \frac{2}{3} - 2z \ln \frac{Q^2}{z} + \frac{4}{3} + \frac{20}{3} z \ln \left(\frac{Q^2}{z} - z \right) - \frac{4}{3} + \frac{52}{3} z \ln \frac{1+b(\))}{2} \\
& + \frac{2}{3} + \frac{26}{3} z \ln(1-z) - 2 + \frac{46}{3} z \ln z + \frac{13}{3} - \frac{55}{3} z + b(\)) - \frac{16}{3} \frac{z}{Q^2} \\
& \frac{2}{1-z} - \frac{1}{6z} - \frac{8}{3} \frac{z^2}{Q^4} \frac{1}{1-z} - 9z \ln^h \frac{Q^2}{z} - z \frac{(1-z)^h}{z^2} \\
& + \frac{8}{3} \frac{z}{Q^2} \frac{7}{1-z} - 12 + 9z \frac{1}{(1-z)^2} - \frac{2}{3} \frac{z^2}{Q^4} \frac{2}{(1-z)^2} + \frac{18}{1-z} \\
& 36 + \frac{1}{(1-z)^2} + \frac{8}{9} b(\)) b^2(\)) - 1) + \frac{40}{9} (1-b) 1+z - \frac{2}{1-z} \\
& \ln^h \frac{Q^2}{z} - z \frac{(1-z)^h}{z^2} + \frac{4}{27} b(\)) (1-b^2(\)) - 10 + 28z - \frac{17}{1-z} \\
& + (1-b(\)) - \frac{344}{27} - \frac{704}{27} z + \frac{628}{27} \frac{1}{1-z} \tag{A.8}
\end{aligned}$$

respectively. As has been mentioned below Eq. (3) the expressions above are finite in the limit $m \rightarrow 0$ ($b \neq 1$) so that they do not contain collinear divergences.

References

- [1] E.W. Itten, Nucl. Phys. B 104, 445 (1976).
 J. Babcock and D. Sivers, Phys. Rev. D 18, 2301 (1978).
 M. A. Shifman, A. I. Vainstein and V. J. Zakharov, Nucl. Phys. B 136, 157 (1978).
 M. G. Luck and E. Reya, Phys. Lett. B 83, 98 (1979).
 J. V. Leveille and T. W. Eiler, Nucl. Phys. B 147, 147 (1979).
- [2] J. Breitweg et al. (ZEUS Collaboration), Phys. Lett. B 407, 402 (1997), hep-ex/9908012.
- [3] C. Adlo et al. (H1-collaboration), Nucl. Phys. B 545, 21 (1999).
- [4] M. G. Luck, E. Reya and M. Stratmann, Nucl. Phys. B 422, 37 (1994);
 A. Vogt in Deep Inelastic Scattering and Related Phenomena, DIS96, edited by G. D'Agozini and A. Nigro, (World Scientific 1997), p. 254, hep-ph/9601352.
- [5] E. Laenen, S. Riemersma, J. Smith and W. L. van Neerven, Nucl. Phys. B 392, 162 (1993); ibid. 229 (1993).
 S. Riemersma, J. Smith and W. L. van Neerven, Phys. Lett. B 347, 43 (1995).
 B. W. Harris and J. Smith, Nucl. Phys. B 452, 109 (1995).
- [6] M. Buza, Y. M. Atouine, J. Smith, W. L. van Neerven, Eur. Phys. J. C 1, 301 (1998).
- [7] M. A. G. Aivazis, J.C. Collins, F. I. Olness and W.-K. Tung, Phys. Rev. D 50, 3102 (1994); F. Olness and S. Riemersma, Phys. Rev. D 51, 4746 (1995).
- [8] J.C. Collins, Phys. Rev. D 58, 0940002 (1998).
- [9] M. Buza, Y. M. Atouine, J. Smith, W. L. van Neerven, Phys. Lett. B 411, 211 (1997); W. L. van Neerven, Acta Phys. Polon. B 28, 2715 (1997); W. L. van Neerven in Proceedings of the 6th International Workshop on Deep Inelastic Scattering and QCD "DIS98" edited by G. H. Corrigan and R. Roosen, (World Scientific, 1998), p. 162-166, hep-ph/9804445;

J. Smith in *New Trends in HERA Physics*, edited by B.A. Kniehl, G. Kramer and A. Wagner, (World Scientific, 1998), p. 283, hep-ph/9708212.

[10] R.S. Thorne and R.G. Roberts, *Phys. Lett. B* 421, 303 (1998); *Phys. Rev. D* 57, 6871 (1998).

[11] M. Glück, E. Reya and A. Vogt, *Eur. Phys. J. C* 5, 461 (1998).

[12] W. L. van Neerven and E.B. Zijlstra, *Phys. Lett. B* 272, 127 (1991), E.B. Zijlstra and W. L. van Neerven, *Phys. Lett. B* 273, 476 (1991), *Nucl. Phys. B* 383, 525 (1992).

[13] P.J. Rijken and W. L. van Neerven, *Phys. Rev. D* 51, 44 (1995).

[14] M. Buza, Y.M. Atoumiane, J. Smith, R. Migneron and W. L. van Neerven, *Nucl. Phys. B* 472, 611 (1996).

[15] W. L. van Neerven and J.A.M. Vermaasen, *Nucl. Phys. B* 238, 73 (1984); See also S. Ketzer and I. Schienbein, *Phys. Rev. D* 58, 094035 (1998).

[16] F.A. Berends, G.J.J. Burgers and W. L. van Neerven, *Nucl. Phys. B* 297, 429 (1988); Erratum *ibid. Nucl. Phys. B* 304, 921 (1988).

[17] A.D. Martin, R.G. Roberts, W.J. Stirling and R. Thorne, *Eur. Phys. J. C* 4, 463 (1998).

[18] H.L. Lai, J. Huston, S. Kuhlmann, J. Moron, F. Olness, J. Owens, J. Pumplin, W.K. Tung, hep-ph/9903282.

[19] S.A. Larin, T. van Ritbergen and J.A.M. Vermaasen, *Nucl. Phys. B* 427, 41 (1994); S.A. Larin et al., *Nucl. Phys. B* 492, 338 (1997).

[20] W. L. van Neerven and A. Vogt, hep-ph/9907472

[21] A. Chuvakin and J. Smith, in preparation.

[22] M. Botje, *QCDNUM 16: A fast QCD evolution program*, *Zeus Note* 97-066.

[23] J. Blumlein, S. Riemersma, W. L. van Neerven and A. Vogt, Nucl. Phys. B (Proc. Suppl.) 51C, 96 (1996);
J. Blumlein et al., in Proceedings of the Workshop on Future Physics at HERA edited by G. Ingelman, A. De Roeck and R. Kanner, Hamburg, Germany, 25-26 Sep. 1995, p. 23, DESY 96-199, hep-ph/9609400.

Figure Captions

Fig. 1. The lowest-order photon-gluon fusion process $\gamma + g \rightarrow Q + Q$ contributing to the coefficient functions $H_{i,g}^{S;(1)}$.

Fig. 2. Some virtual gluon corrections to the process $\gamma + g \rightarrow Q + Q$ contributing to the coefficient functions $H_{i,g}^{S;(2)}$.

Fig. 3. The bremsstrahlung process $\gamma + g \rightarrow Q + Q + g$ contributing to the coefficient functions $H_{i,g}^{S;(2)}$.

Fig. 4. The Bethe-Heitler process $\gamma + q(q) \rightarrow Q + Q + q(q)$ contributing to the coefficient functions $H_{i,q}^{PS;(2)}$. The light quarks q and the heavy quarks Q are indicated by dashed and solid lines respectively.

Fig. 5. The Compton process $\gamma + q(q) \rightarrow Q + Q + q(q)$ contributing to the coefficient functions $L_{i,q}^{NS;(2)}$. The light quarks q and the heavy quarks Q are indicated by dashed and solid lines respectively ($s = (p + q)^2$, $s_{QQ} = (p_1 + p_2)^2$ see text).

Fig. 6. The two-loop vertex correction to the process $\gamma + q \rightarrow q$ containing a heavy quark (Q) loop. It contributes to $C_{i,q}^{VIRT NS;(2)}(Q^2=m^2) = F^{(2)}(Q^2=m^2) C_{i,q}^{(0)}$.

Fig. 7. Order ϵ corrections to the process $\gamma + Q \rightarrow Q$ and the reaction $+ Q \rightarrow Q + g$ contributing to the coefficient functions $H_{i,Q}^{NS;(1)}$.

Fig. 8. The $\epsilon = (s - 4m^2)/(s + 4m^2)$ dependence of $xL_{2,q}^{SOFT NS;(2)}(x; Q^2=m^2)$ at $Q^2=m^2 = 50$ (Eq. (A 2)) plotted as a function of x for $\epsilon = 1, 0.1, 0.01$ and 0.001 respectively.

Fig. 9. (a) The charm density $xC^{NNLO}(4; x; Q^2)$ shown in the range $10^{-5} < x < 1$ for $Q^2 = 1.96, 2.0, 3.0, 4.0, 5.0, 10$ and 100 in units of $(GeV=c)^2$. (b) similar plot as in (a) but now for $0.01 < x < 1$. For a comparison we have also shown the NLO results obtained by MRS 98 and CTEQ 5HQ for the range $10^{-5} < x < 1$ in (c) and (d) respectively.

Fig. 10. Ratios $R(x; Q^2) = xC^{EVOLVED}(4; x; Q^2)/xC^{FOPT}(4; x; Q^2)$ for the scales $Q^2 = 2.0, 3.0, 4.0, 5.0, 10, 100$ in units of $(GeV=c)^2$. (a) LO, (b) NLO, (c) NNLO.

Fig. 11. The charm quark structure functions $F_{2;c}^{\text{EXACT}} (n_f = 3)$ (solid line) $F_{2;c}^{\text{VFNS}} (n_f = 4)$, (dot-dashed line) $F_{2;c}^{\text{BM SN}} (n_f = 4)$, (dashed line) and $F_{2;c}^{\text{PDF}} (n_f = 4)$, (dotted line) in NNLO for $x = 0.05$ plotted as functions of Q^2 .

Fig. 12. Same as in Fig. 11 but now for $x = 0.005$.

Fig. 13. The charm quark structure functions $F_{L;c}^{\text{EXACT}} (n_f = 3)$ (solid line) $F_{L;c}^{\text{VFNS}} (n_f = 4)$, (dot-dashed line) $F_{L;c}^{\text{BM SN}} (n_f = 4)$, (dashed line) and $F_{L;c}^{\text{PDF}} (n_f = 4)$, (dotted line) in NNLO for $x = 0.05$ plotted as functions of Q^2 .

Fig. 14. Same as in Fig. 13 but now for $x = 0.005$.

Fig. 15. The charm quark structure functions $F_{2;c}^{\text{BM SN}} (n_f = 4)$ in NLO (solid line), NNLO (dotted line) for $x = 0.05$ and $F_{2;c}^{\text{VFNS}} (n_f = 4)$ in NLO (dashed line), NNLO (dot-dashed line) for $x = 0.05$ plotted as functions of Q^2 .

Fig. 16. Same as in Fig. 15 but now for $x = 0.005$.

Fig. 17. The charm quark structure functions $F_{L;c}^{\text{BM SN}} (n_f = 4)$ in NLO (solid line), NNLO (dotted line) for $x = 0.005$ and $F_{L;c}^{\text{VFNS}} (n_f = 4)$ in NLO (dashed line), NNLO (dot-dashed line) for $x = 0.05$ plotted as functions of Q^2 .

Fig. 18. Same as in Fig. 17 but now for $x = 0.005$.

Fig 8

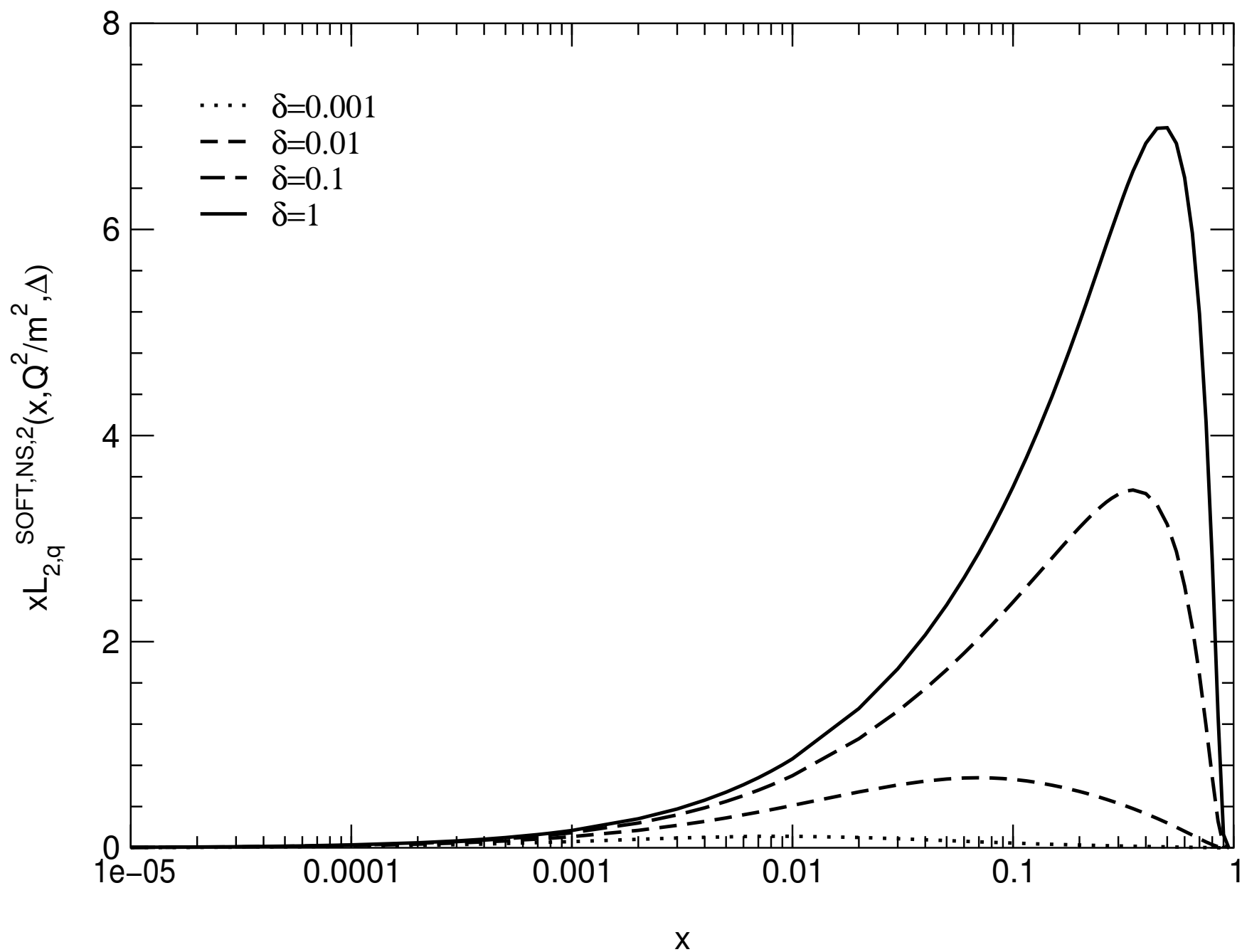


Fig 9(a)

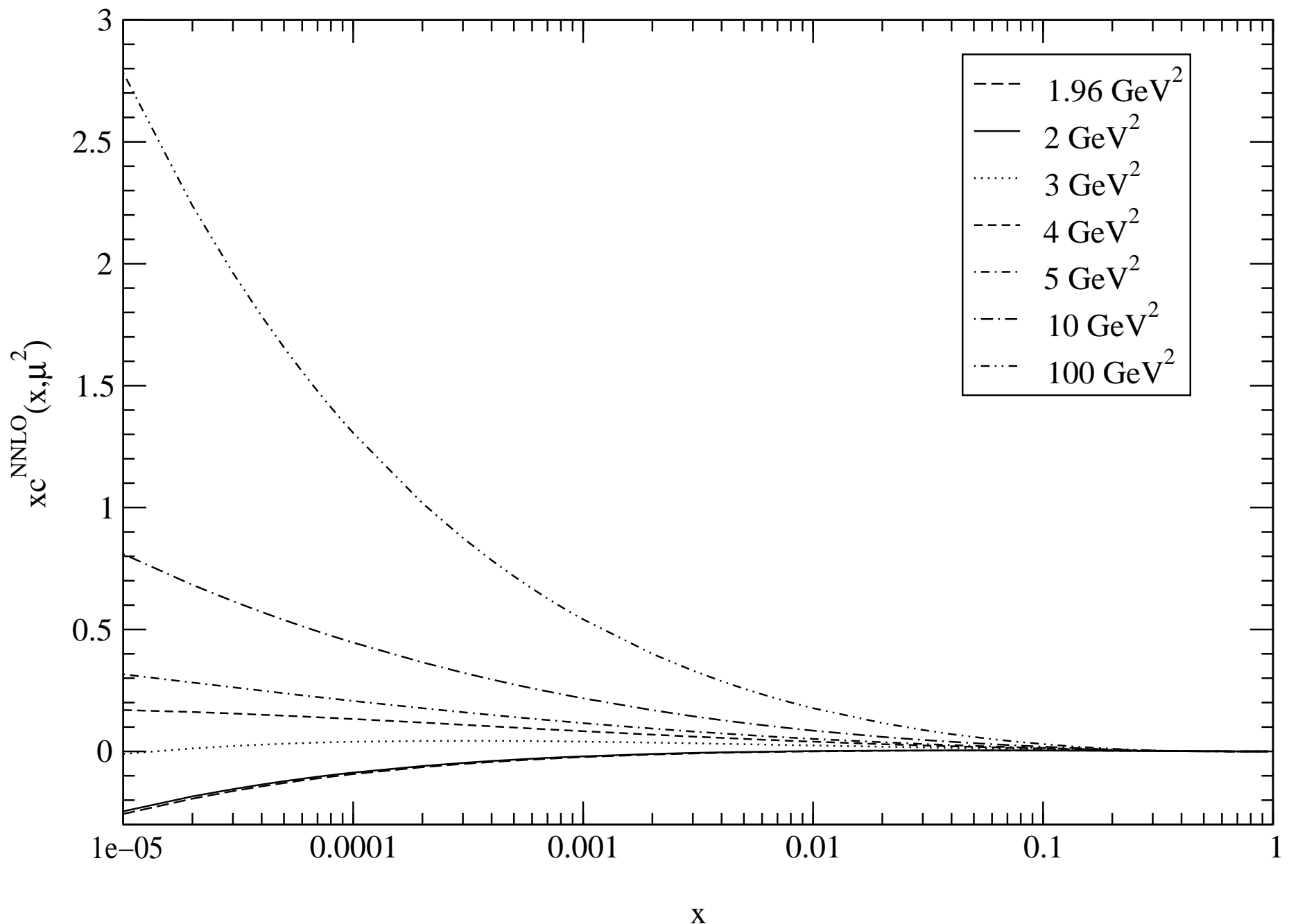


Fig 9(b)

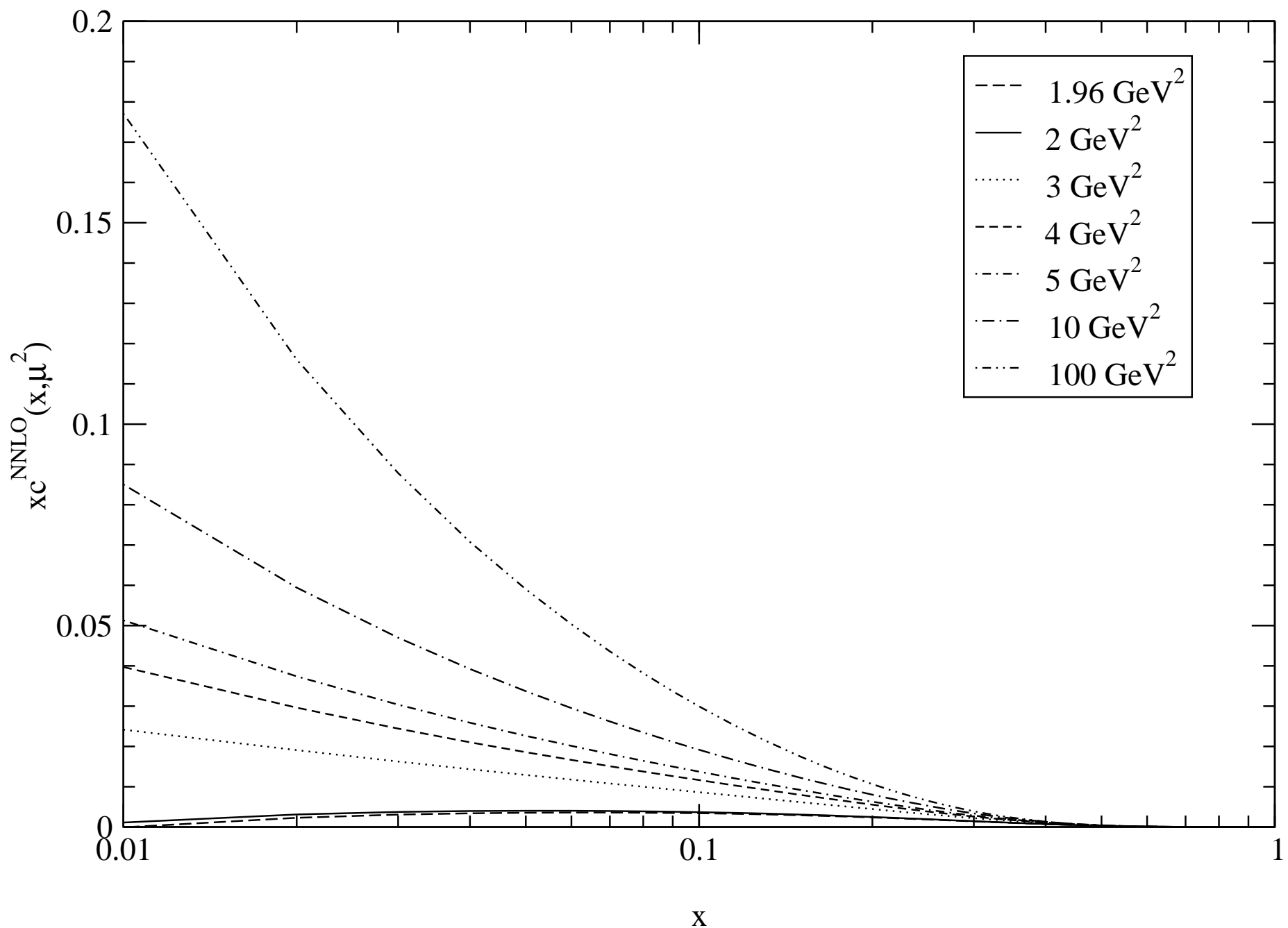


Fig 9(c)

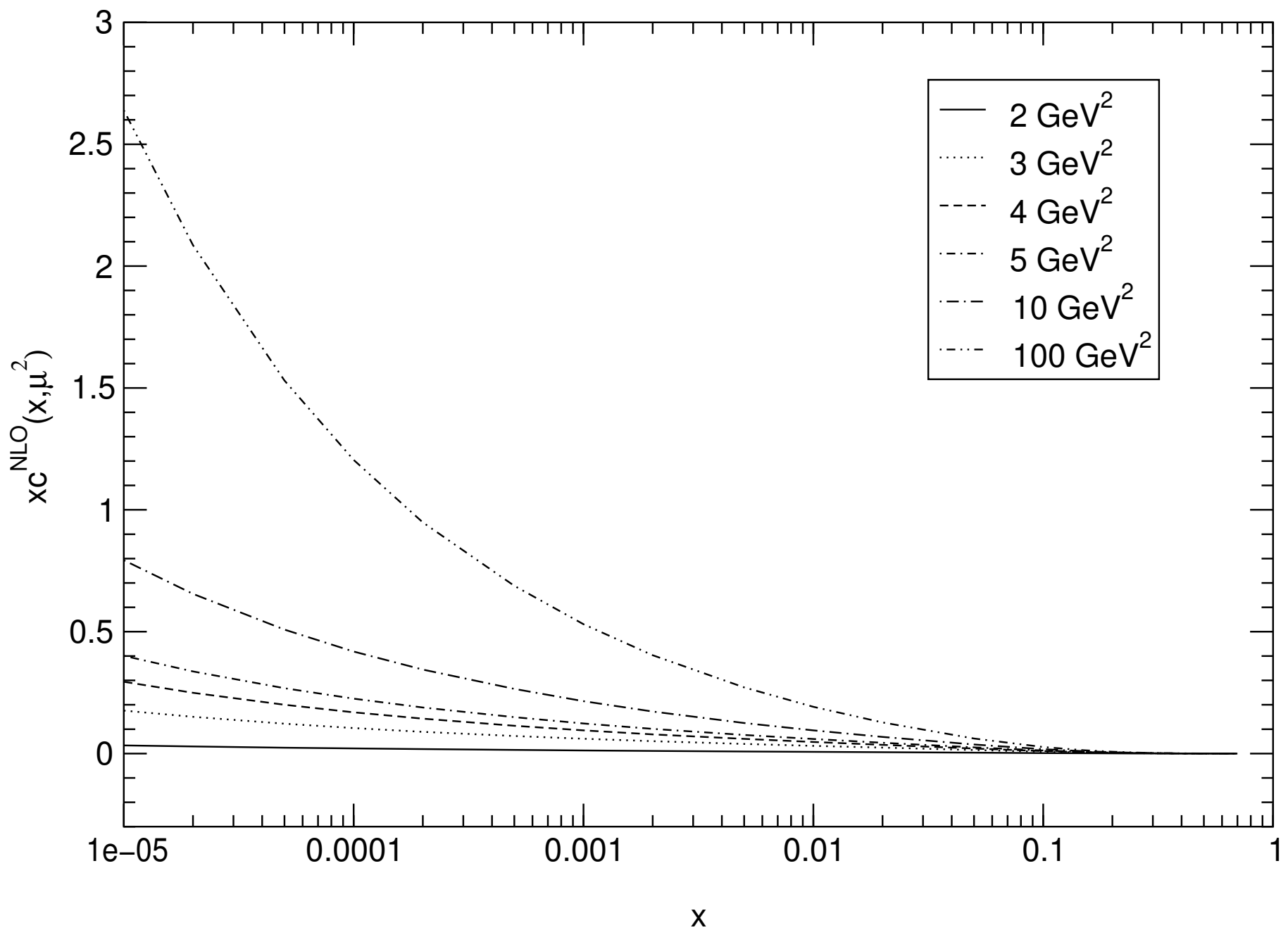


Fig 9(d)

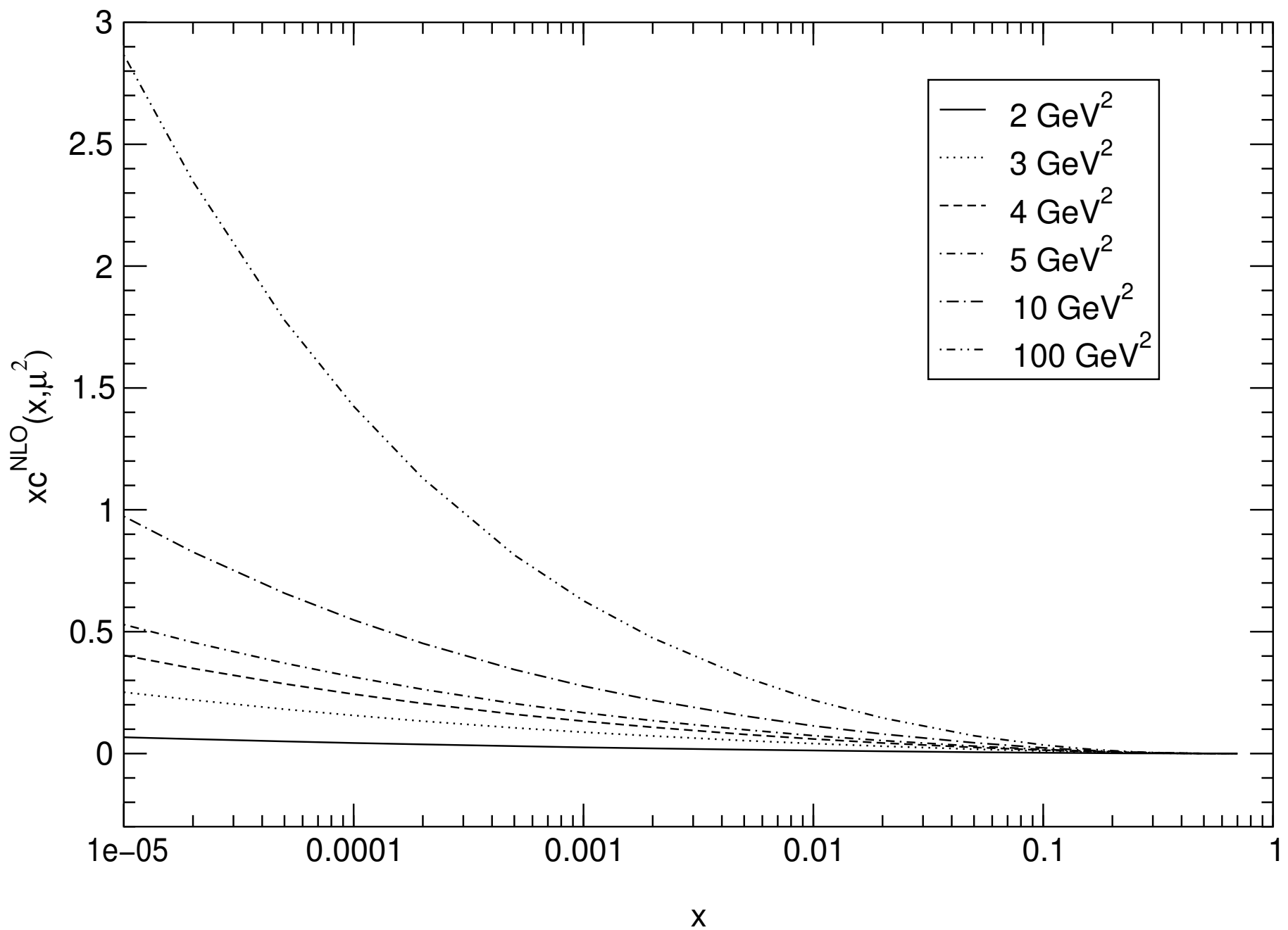


Fig 10(a)

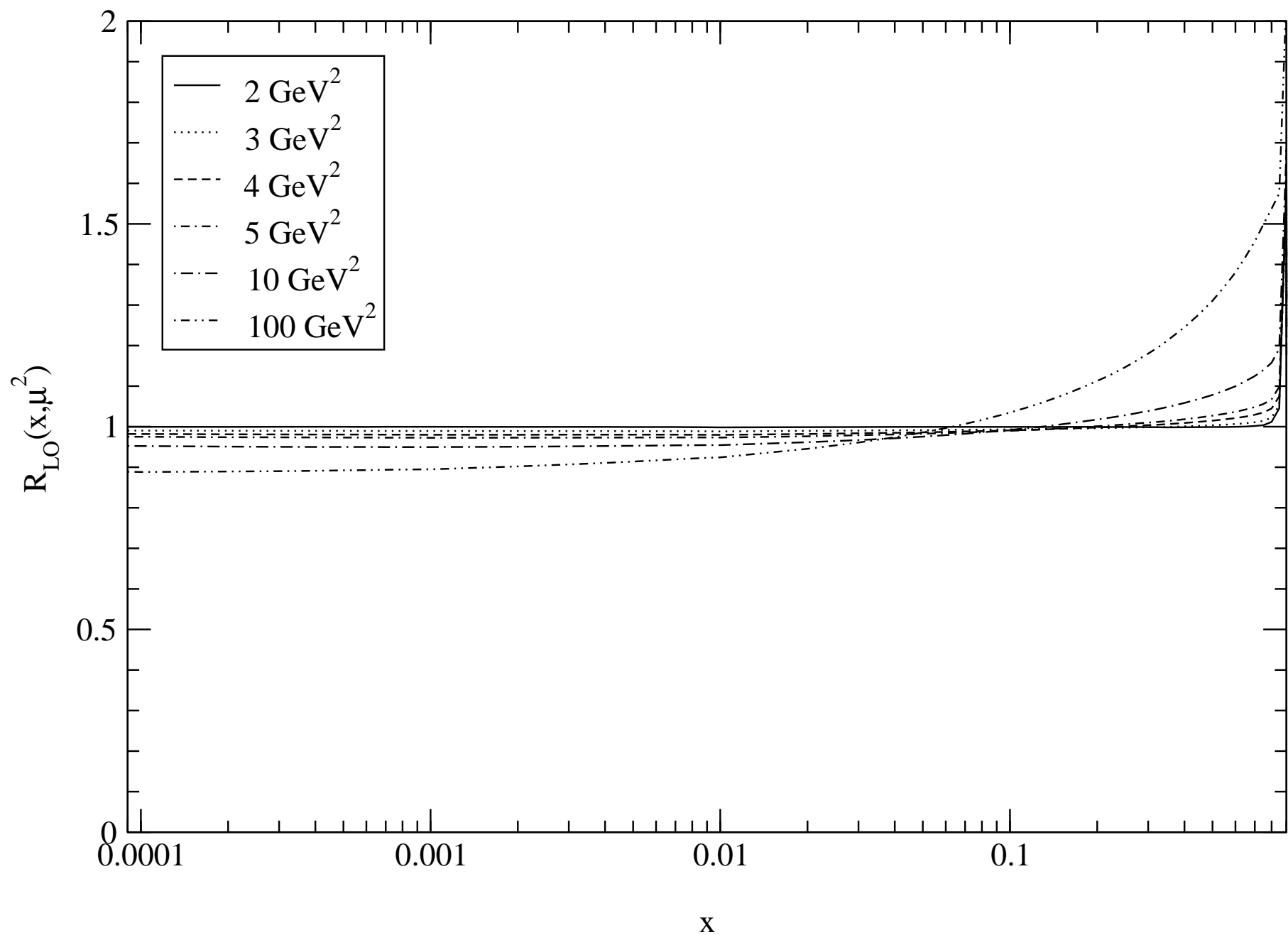


Fig 10(b)

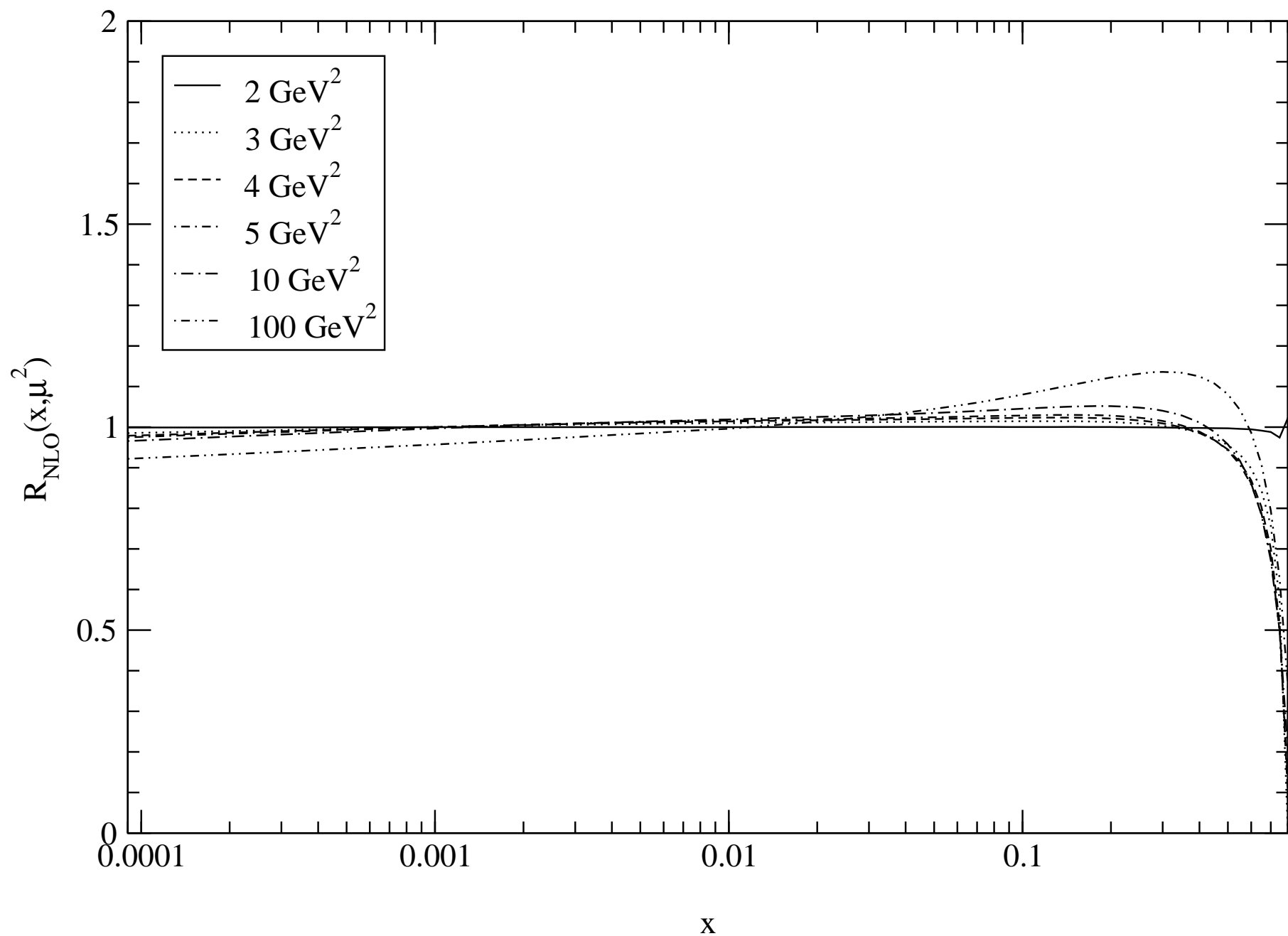


Fig 10(c)

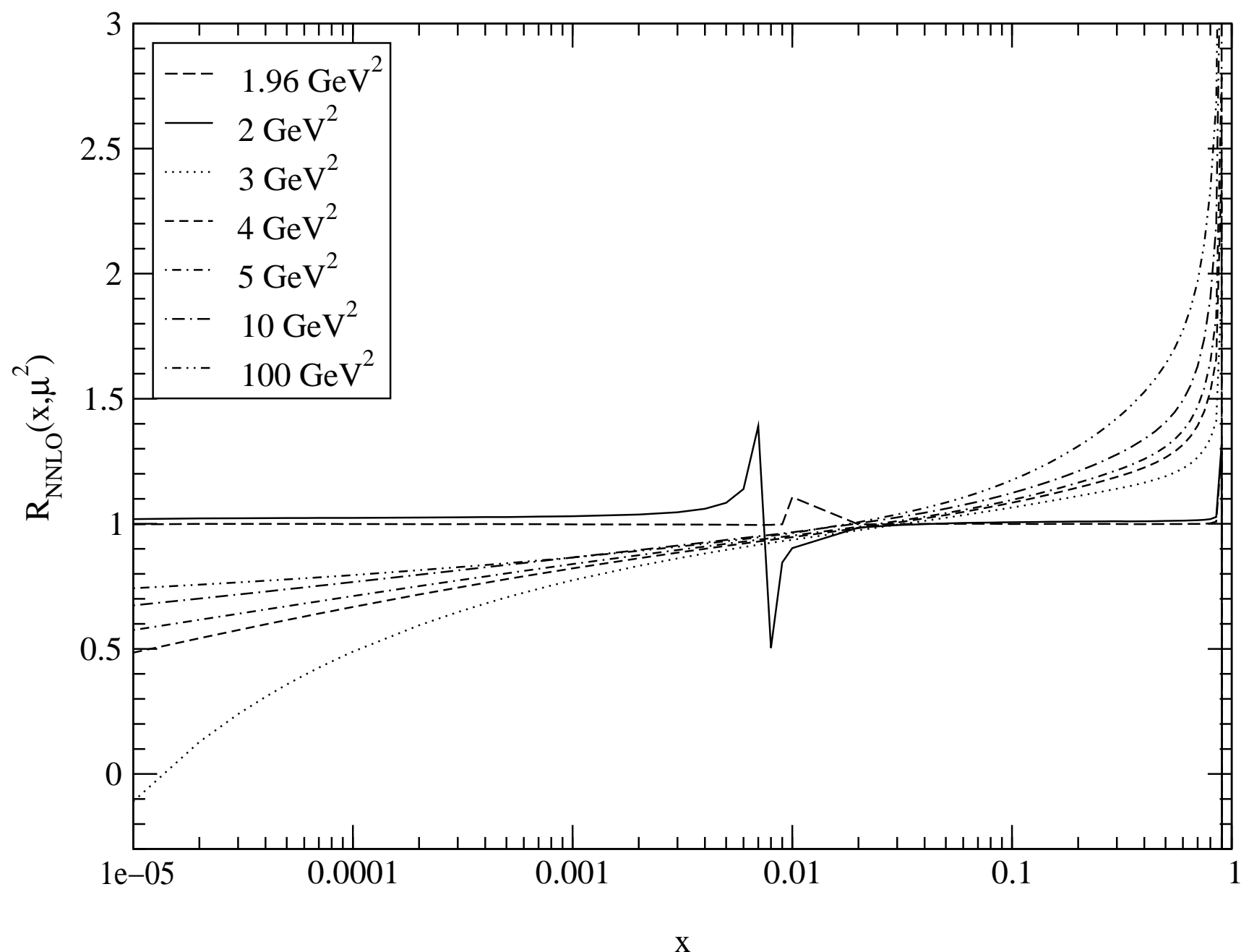


Fig 11

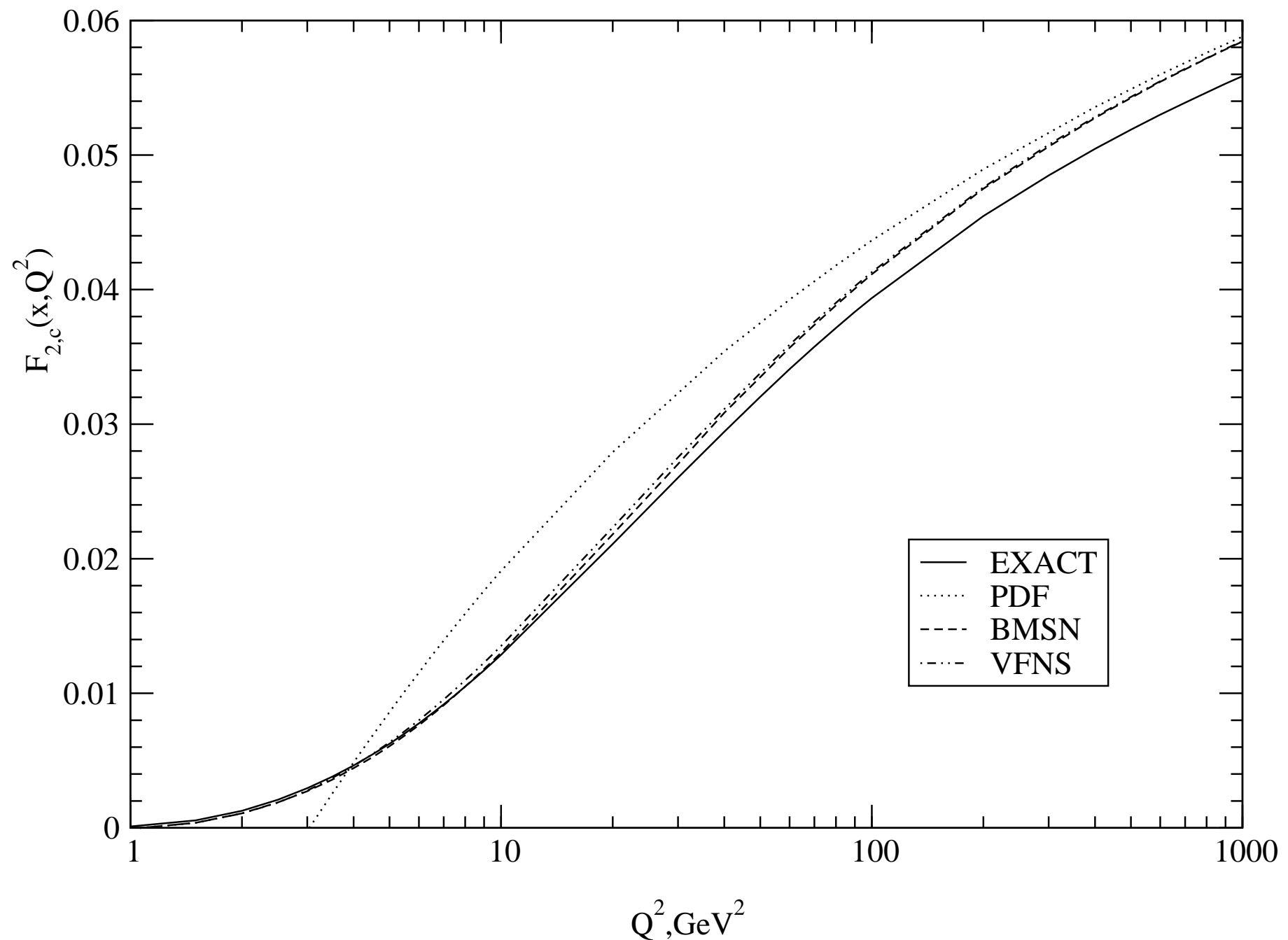


Fig 12

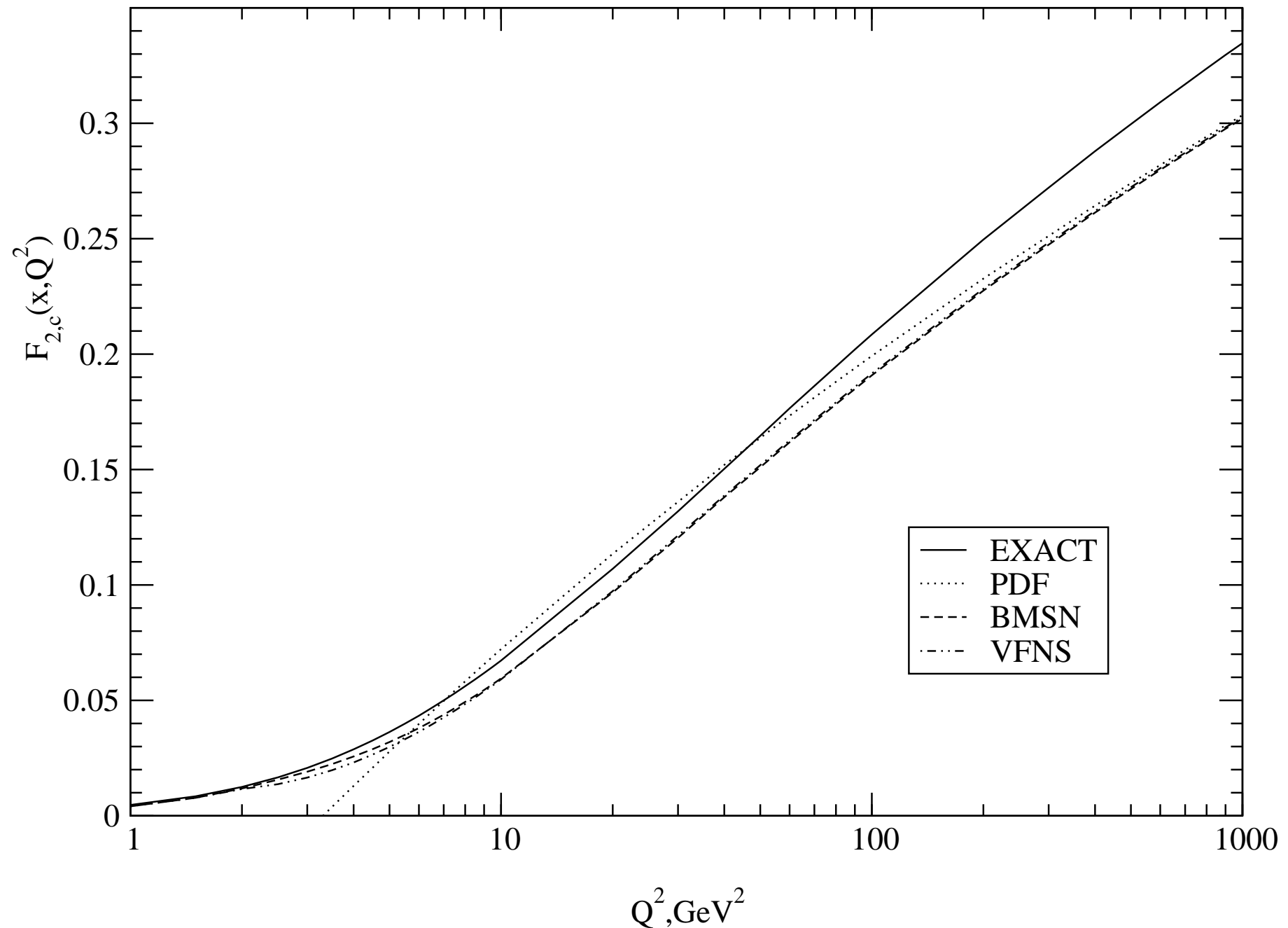


Fig 13

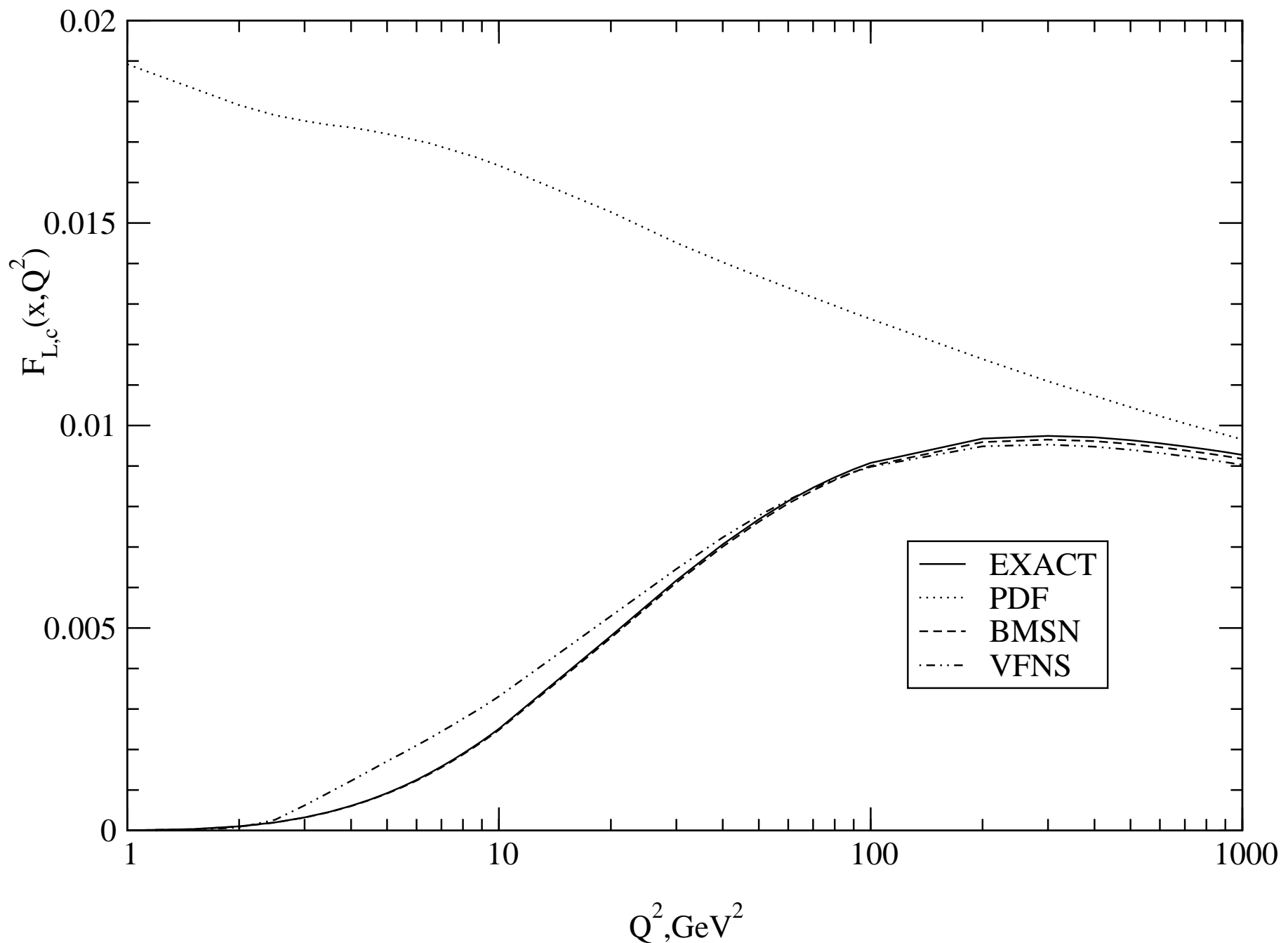


Fig 14

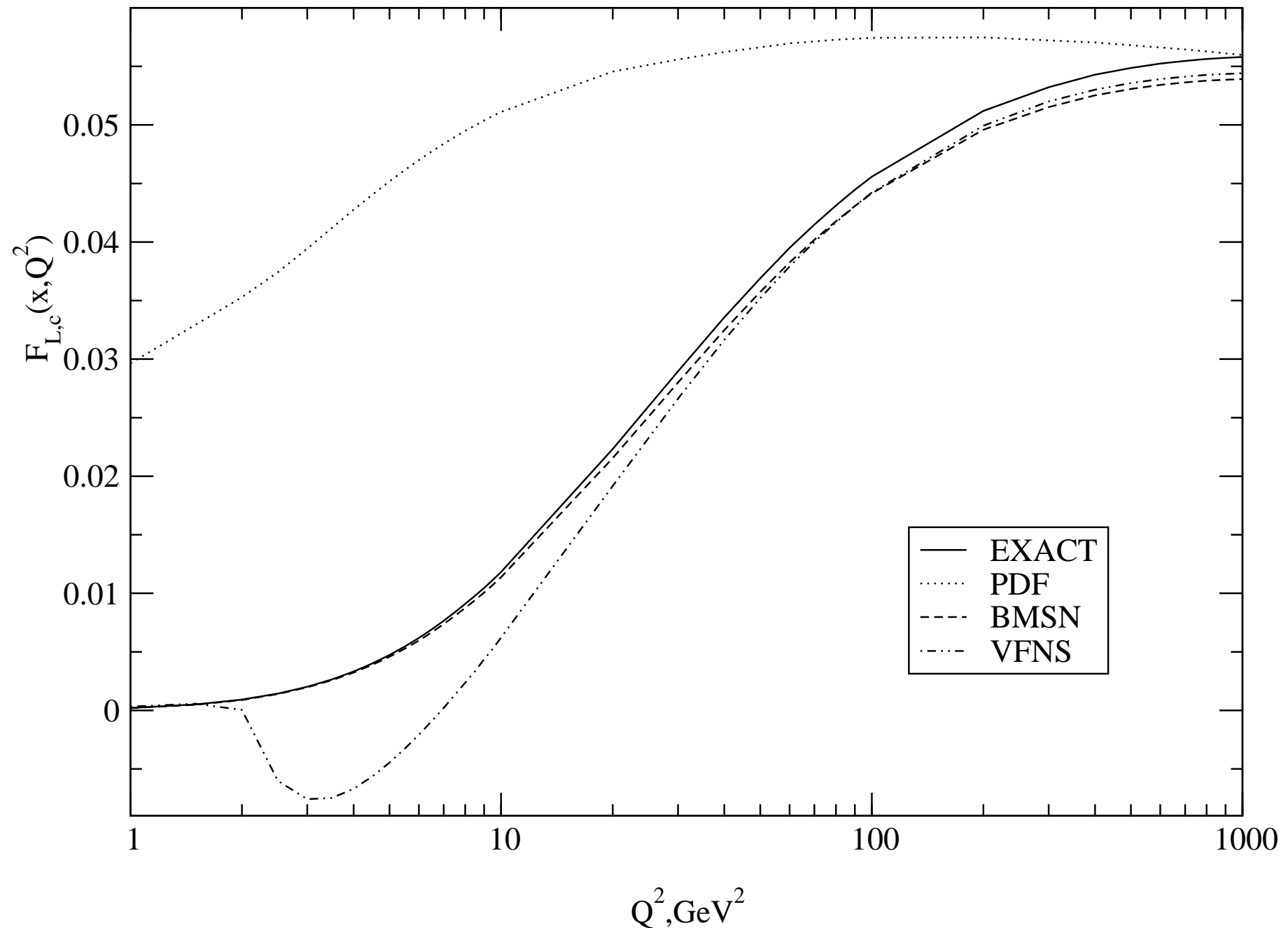


Fig 15

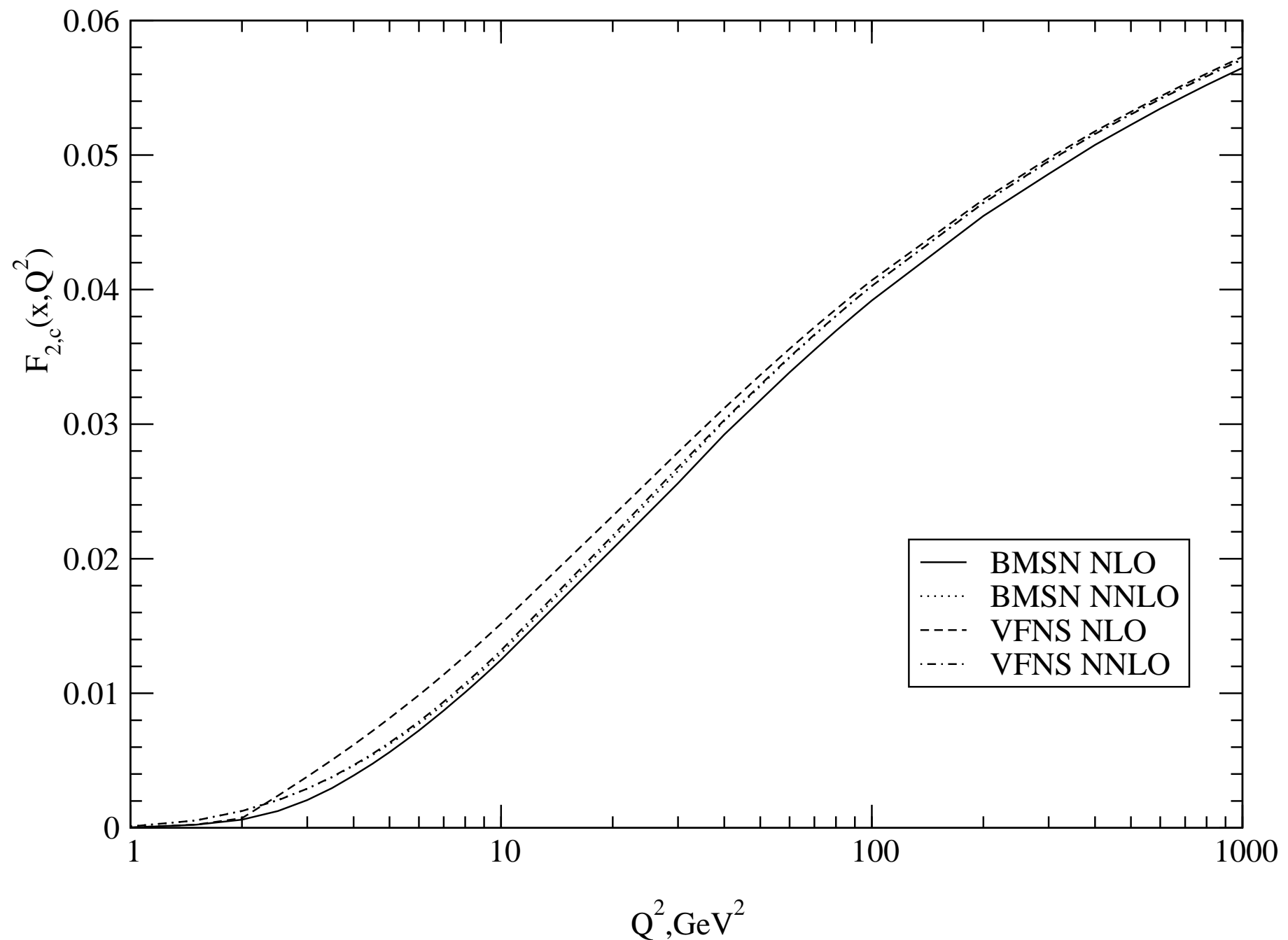


Fig 16

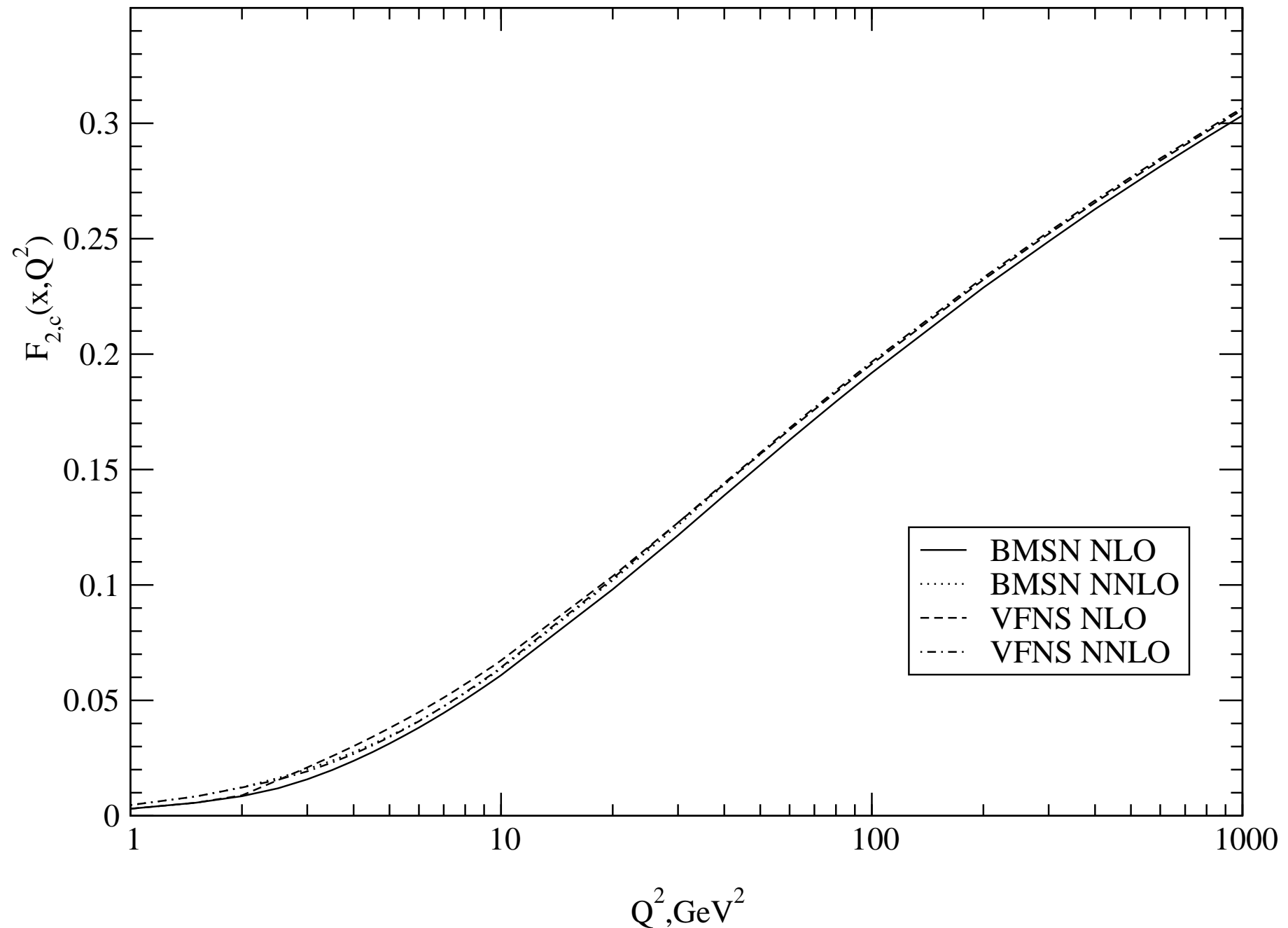


Fig 17

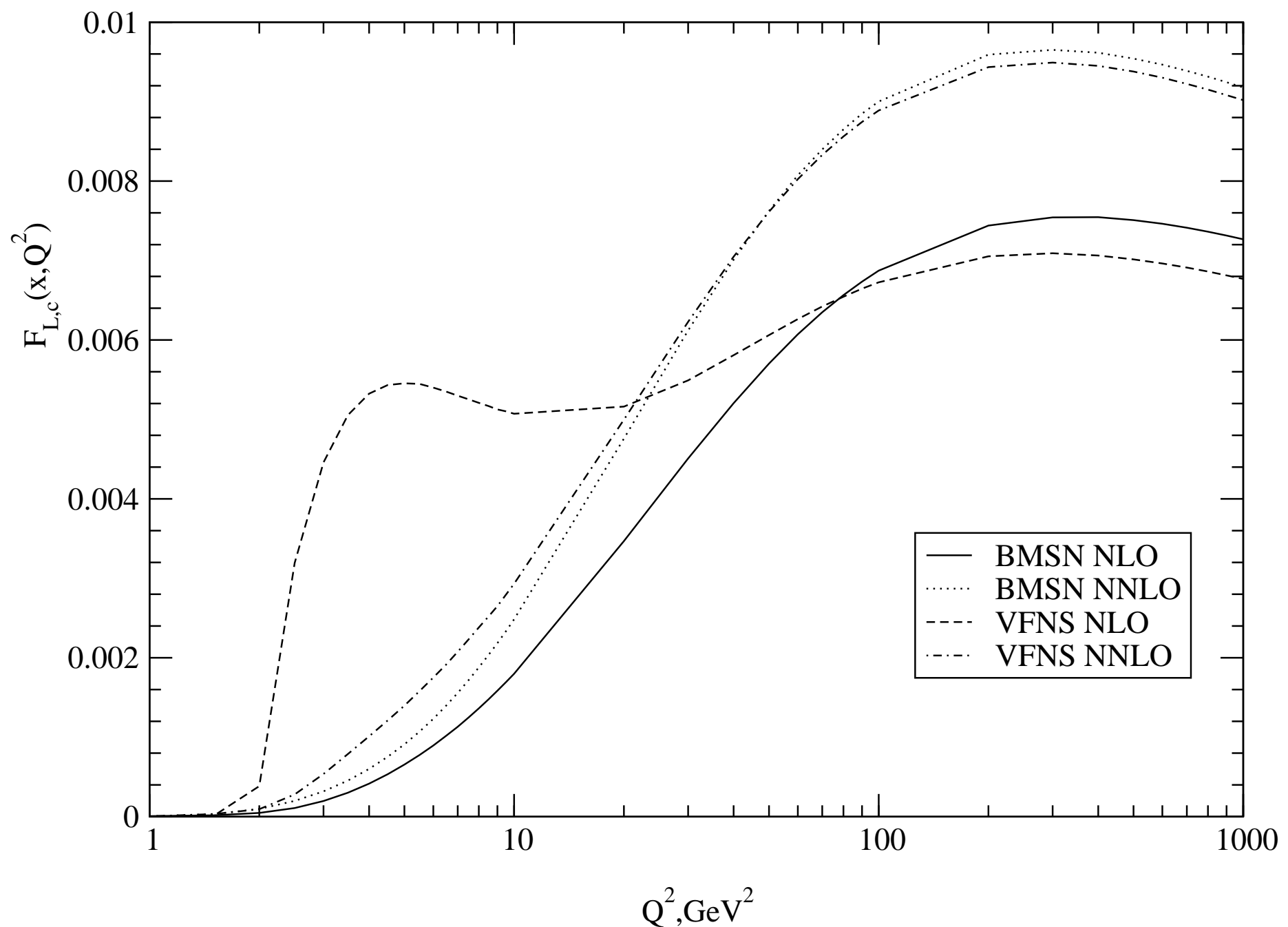


Fig 18

